



# AN ABSTRACT OF THE DISSERTATION OF

Zhian N. Kamvar for the degree of Doctor of Philosophy in Botany and Plant Pathology presented on December 6, 2016.

Title: Development and Application of Tools for Analysis of Clonal Population Genetics

Abstract approved: \_\_\_\_\_

Niklaus J. Grünwald

This is a  $\text{\LaTeX}$  template derived from the  $\text{\LaTeX}$  template found on overleaf (<https://www.overleaf.com/latex/templates/oregon-state-university-thesis-and-dissertation/wnvzcdhqshxf>) and cloned using git clone <https://git.overleaf.com/5973847rnpkdf> I have made the following changes

- modified beavtex.cls from v1.1 to include support for verbatim font styles in R code
- stripped the template of its original content to create a pandoc template
- placed this into a bookdown (<https://bookdown.org/>) framework
- added packages latexsym, amsmath amssymb,amsthm, longtable, booktabs, setspace, url, hyperref, lmodern, caption, and float

This is still a WIP, but it seems to work for the moment. Zhian N. Kamvar 2016-

©Copyright by Zhian N. Kamvar  
December 6, 2016  
All Rights Reserved

Development and Application of Tools for Analysis of Clonal Population  
Genetics

by

Zhian N. Kamvar

A DISSERTATION

submitted to

Oregon State University

in partial fulfillment of  
the requirements for the  
degree of

Doctor of Philosophy

Presented December 6, 2016  
Commencement June 2017

Doctor of Philosophy dissertation of Zhian N. Kamvar presented on  
December 6, 2016.

APPROVED:

---

Major Professor, representing Botany and Plant Pathology

---

Head of the Department of Botany and Plant Pathology

---

Dean of the Graduate School

I understand that my dissertation will become part of the permanent collection of Oregon State University libraries. My signature below authorizes release of my dissertation to any reader upon request.

---

Zhian N. Kamvar, Author

## ACKNOWLEDGEMENTS

I would like to acknowledge... Lorem ipsum dolor sit amet, consectetur adipiscing elit. Maecenas vel eros sed mauris porttitor semper nec a orci. Nullam vestibulum mi nec condimentum posuere. Pellentesque eget diam id sapien aliquet ullamcorper. Pellentesque blandit nec lectus ut mollis. Praesent in facilisis justo. Vestibulum ante ipsum primis in faucibus orci luctus et ultrices posuere cubilia Curae; Sed eget congue leo, sed consequat libero. In rutrum malesuada nisi. Vestibulum ante ipsum primis in faucibus orci luctus et ultrices posuere cubilia Curae; Morbi sollicitudin tortor ut sem facilisis mollis.

## CONTRIBUTION OF AUTHORS

The following people contributed to this dissertation:

### Chapter 2

Javier F. Tabima assisted in writing the code and design, Niklaus J. Grünwald assisted in design, and editing of the manuscript.

### Chapter 3

Zhian N. Kamvar, Meredith M. Larsen, Alan M. Kanaskie, Everett M. Hansen, and Niklaus J. Grünwald . . .

### Chapter 4

Jonah C. Brooks assisted in writing and testing the code. Niklaus J. Grünwald assisted in the design, coördination of the collaborative effort, and editing the manuscript.

### Chapter 5

Niklaus J. Grünwald assisted in the design, and editing of the manuscript.

## TABLE OF CONTENTS

	<u>Page</u>
1 Introduction . . . . .	1
1.1 Population genetics of clonal organisms . . . . .	1
1.2 The Genus <i>Phytophthora</i> . . . . .	2
1.2.1 life cycle . . . . .	2
1.2.2 Sex and mating types . . . . .	2
1.2.3 Heterothallic, clonal: <i>P. ramorum</i> . . . . .	2
1.2.4 Homothallic, partially clonal: <i>P. syringae</i> . . . . .	3
1.3 Tools for analysis of clonal population genetics . . . . .	3
1.3.1 Index of Association . . . . .	3
1.3.2 Software Limitations . . . . .	4
1.3.3 poppr . . . . .	4
1.4 Applications of novel tools for analysis of partially-clonal populations . . . . .	4
1.5 Conclusion . . . . .	4
2 <i>Poppr</i> : an R Package For Genetic Analysis of Populations With Clonal, Partially Clonal, and/or Sexual Reproduction . . . . .	6
2.1 Abstract . . . . .	7
3 Novel R Tools For Analysis of Genome-Wide Population Genetic Data With Emphasis on Clonality . . . . .	8
3.1 Abstract . . . . .	9
3.2 Introduction . . . . .	9
3.3 Implementations and Examples . . . . .	12
3.3.1 Clonal identification . . . . .	12
3.3.2 Minimum Spanning Networks with Reticulation . . . . .	19
3.3.3 Bootstrapping . . . . .	22
3.3.4 Genotype Accumulation Curve . . . . .	24
3.3.5 Index of association . . . . .	27
3.3.6 Data format updates: population strata and hierarchies . . . . .	29

## TABLE OF CONTENTS (Continued)

	<u>Page</u>
3.4 Availability . . . . .	31
3.4.1 Requirements . . . . .	31
3.4.2 Installation . . . . .	32
3.5 Discussion . . . . .	32
3.6 Acknowledgements . . . . .	35
4 Spatial and Temporal Analysis of Populations of the Sudden Oak Death Pathogen in Oregon Forests . . . . .	36
4.1 Abstract . . . . .	37
4.2 Introduction . . . . .	37
4.3 Materials and Methods . . . . .	39
4.3.1 Location . . . . .	39
4.3.2 Sampling . . . . .	42
4.3.3 Isolation, identification and DNA extraction . . . . .	42
4.3.4 Genotyping, data validation, and harmonization . . . . .	44
4.3.5 Nursery populations . . . . .	47
4.3.6 Data analysis . . . . .	47
4.4 Results . . . . .	51
4.4.1 Demographic pattern and genetic diversity . . . . .	51
4.4.2 Spatial Correlation . . . . .	55
4.4.3 Population differentiation . . . . .	55
4.4.4 Clustering of forest with nursery populations . . . . .	60
4.5 Discussion . . . . .	62
4.6 Acknowledgements . . . . .	66
4.7 Supplementary Material . . . . .	67
4.7.1 Supplementary Text . . . . .	67
4.7.2 Supplementary Figures . . . . .	70
5 [Tentative Title] Population Dynamics of the Plant Pathogen <i>Phytophthora syringae</i> in Oregon Nurseries . . . . .	79
5.1 Abstract . . . . .	79

## TABLE OF CONTENTS (Continued)

	<u>Page</u>
5.2 Introduction . . . . .	79
6 [Tentative Title] The Effect of Population Dynamics, Sample Size, and Marker Choice on the Index of Association . . . . .	80
6.1 Abstract . . . . .	81
6.2 Introduction . . . . .	81
6.3 Methods . . . . .	85
6.3.1 Simulating Microsatellite Loci . . . . .	86
6.3.2 GBS Simulations . . . . .	86
6.3.3 Sexual Reproduction . . . . .	87
6.3.4 Analysis of Microsatellite Data . . . . .	87
6.3.5 Analysis of SNP Data . . . . .	88
6.3.6 Power Analysis . . . . .	88
Bibliography . . . . .	90

## LIST OF FIGURES

<u>Figure</u>		<u>Page</u>
3.1	Diagrammatic representation of the three clustering algorithms implemented in <code>mlg.filter</code> .	14
3.2	Graphical representation of three different clustering algorithms collapsing multilocus genotypes for 12 SSR loci from <i>Phytophthora infestans</i> representing 18 clonal lineages.	16
3.3	Minimum Spanning Networks with Reticulation	21
3.4	UPGMA dendrogram generated from Nei's genetic distance	24
3.5	Genotype accumulation curve	26
3.6	Sliding window analysis of the standardized index of association ( $\bar{r}_d$ )	29
4.1	Spatial distribution of the SOD epidemic and multilocus genotypes of <i>Phytophthora ramorum</i> in Curry County, Oregon.	41
4.2	Rank distribution of multilocus genotypes (MLGs) of <i>P. ramorum</i> and recovery per year.	52
4.3	Minimum spanning network based on Bruvo's genetic distance for microsatellite markers for <i>P. ramorum</i> populations.	54
4.4	Scatterplot from DAPC of the first two principal components discriminating <i>P. ramorum</i> populations by regions.	59
4.5	Unrooted, neighbor-joining tree with 10,000 bootstrap replicates of Nei's genetic distance for <i>P. ramorum</i> populations defined by region.	61
4.6	Diagram of DNA extraction, genotyping, and sequencing protocols utilized by two labs from 2001 to 2014.	70
4.7	Genotype accumulation curve for OR forest <i>P. ramorum</i> isolates.	71
4.8	Neighbor joining tree based on Nei's distance of the forest <i>P. ramorum</i> isolates by region with respect to year.	72
4.9	Fractions of posterior population assignments from DAPC clustering of <i>P. ramorum</i> isolates from forest populations.	73

## LIST OF FIGURES (Continued)

<u>Figure</u>	<u>Page</u>
4.10 Loading plot from DAPC of <i>P. ramorum</i> from forest populations showing the contribution of alleles to the first DAPC eigenvalue separating Hunter Creek isolates from all other regions. . . . .	73
4.11 Prediction of nursery genotypes of <i>P. ramorum</i> into forest watershed regions. . . . .	74
4.12 Graphical representation of prediction of nursery isolates of <i>P. ramorum</i> into forest watershed regions. . . . .	75
4.13 Graphical representation of predicted membership of <i>P. ramorum</i> isolates from Hunter Creek and Pistol River South Fork in forest and nursery populations. . . . .	76
4.14 Allele frequencies of locus PrMS39 of <i>P. ramorum</i> across years of the forest populations. . . . .	77
4.15 Map of the infected area in Curry county showing the <i>P. ramorum</i> genotypes at locus PrMS39. . . . .	78

## LIST OF TABLES

<u>Table</u>	<u>Page</u>
3.1 Contingency table comparing multilocus lineages (MLL) . . . . .	17
4.1 Summary of <i>P. ramorum</i> isolates sampled in Oregon forests and multi-locus genotypes (MLG) observed across regions and years. . . . .	43
4.2 Newly multiplexed protocol for <i>P. ramorum</i> primer sequences of simple sequence repeat (SSR) loci and final concentrations used to determine multilocus genotypes for four clonal lineages. . . . .	45
4.3 Caption for Table 4.2 . . . . .	46
4.4 Table of correlation coefficients generated across forest regions and years of <i>P. ramorum</i> isolates using the Mantel test. . . . .	56
4.5 AMOVA table generated comparing <i>P. ramorum</i> isolates for two different hierarchies . . . . .	58

This dissertation is for my grandfather, Franklin Hepner.

## Chapter 1: Introduction

- Plant Pathogens
  - Evolution and Adaptation
  - Understanding clonal population dynamics (*Phytophthora* and *Zymoseptoria* examples)
- Tools for analysis
  - Tools for clonal populations always come after sexual populations
  - We wrote our own tools
- Goals of my work
  1. development of computational tools to characterize populations
  2. application of these tools to address empirical and theoretical questions

### 1.1 Population genetics of clonal organisms

- Population genetics is traditionally centered around HWE
- Clonal populations violate basic statistical inference
  - non-independent samples (clones)
  - excess heterozygosity

- Meselson effect (Balloux et al., 2003; Butlin, 2000; Welch and Meselson, 2000, 2001)

## 1.2 The Genus *Phytophthora*

The genus *Phytophthora*, translating to “plant destroyer” in Greek, contains over 100 species (Kroon et al., 2012), many of which have significant impact on US agriculture. *P. sojae* is a major problem on soybean, causing \$1-2 billion in losses each year (Tyler, 2007). *P. ramorum* is changing the landscape of the North American West due to its wide host range (Grünwald et al., 2008a), which results in devastating losses for the US forestry and nursery industries. And *P. infestans*, which was a root cause of over a million deaths during the Irish Potato Famine and continues to be a problem on tomato and potato crops, resulting in losses exceeding \$6 billion, annually (Haas et al., 2009). *Phytophthora spp.* are water molds characterized by production of oospores and biflagellate zoospores that place them into the Stramenopiles (Baldauf, 2003). They are most closely related to golden brown algae and quite diverged from fungi.

### 1.2.1 life cycle

### 1.2.2 Sex and mating types

### 1.2.3 Heterothallic, clonal: *P. ramorum*

- Sudden Oak Death

- Population genetics in US nurseries (Goss et al., 2009)

#### 1.2.4 Homothallic, partially clonal: *P. syringae*

- Abundant in OR Nurseries (found in foliar isolates) (Parke et al., 2014)
- Genetic structure uncharacterized

### 1.3 Tools for analysis of clonal population genetics

Recommendations have been made for analysis (Arnaud-Hanod et al., 2007)

- MLG diversity
- Genotype Accumulation Curve
- $P_{sex}$  and  $P_{gen}$

#### 1.3.1 Index of Association

- Standardized Version (Agapow and Burt, 2001)
- Previous Simulation Analyses (de Meeûs and Balloux, 2004)
- What's missing
  - Sympatric clonal lineages
  - Analysis of significance testing
  - HTS markers

### 1.3.2 Software Limitations

Plethora of tools, most designed for sexual populations except:

- GenClone
- GenoDive

Problems with file formatting, time, and reproducibility.

### 1.3.3 poppr

- R
- poppr

## 1.4 Applications of novel tools for analysis of partially-clonal populations

- Simulation analysis of  $\bar{r}_d$
- SSR analysis of *P. ramorum*
- GBS analysis of *P. syringae*

## 1.5 Conclusion

- Open Source Scientific Software Development of Poppr
  - Related tools
- Simulation Analysis

- Pop gen info for two *Phytophthoras*
- Major results of your work in 2-4 sentences ...

Chapter 2: *Poppr*: an R Package For Genetic Analysis of Populations  
With Clonal, Partially Clonal, and/or Sexual Reproduction

Zhian N. Kamvar, Javier F. Tabima, and Niklaus J. Grünwald

Journal: **PeerJ**

PO Box 614, Corte Madera, CA 94976, USA

Published 2014-03-04, Issue: **2**:e281, DOI: [10.7717/peerj.281](https://doi.org/10.7717/peerj.281)

## 2.1 Abstract

Many microbial, fungal, or oomcyete populations violate assumptions for population genetic analysis because these populations are clonal, admixed, partially clonal, and/or sexual. Furthermore, few tools exist that are specifically designed for analyzing data from clonal populations, making analysis difficult and haphazard. We developed the R package `poppr` providing unique tools for analysis of data from admixed, clonal, mixed, and/or sexual populations. Currently, `poppr` can be used for dominant/codominant and haploid/diploid genetic data. Data can be imported from several formats including GenAIEx formatted text files and can be analyzed on a user-defined hierarchy that includes unlimited levels of subpopulation structure and clone censoring. New functions include calculation of Bruvo's distance for microsatellites, batch-analysis of the index of association with several indices of genotypic diversity, and graphing including dendograms with bootstrap support and minimum spanning networks. While functions for genotypic diversity and clone censoring are specific for clonal populations, several functions found in `poppr` are also valuable to analysis of any populations. A manual with documentation and examples is provided. `Poppr` is open source and major releases are available on CRAN: <http://cran.r-project.org/package=poppr>. More supporting documentation and tutorials can be found under 'resources' at: <http://grunwaldlab.cgrb.oregonstate.edu/>.

## Chapter 3: Novel R Tools For Analysis of Genome-Wide Population Genetic Data With Emphasis on Clonality

Zhian N. Kamvar, Jonah C. Brooks, and Niklaus J. Grünwald

Journal: **Frontiers in Genetics**

EPFL Innovation Park, Building I, CH – 1015 Lausanne Switzerland

Published 2015-06-10. Issue: **6**, DOI: [10.3389/fgene.2015.00208](https://doi.org/10.3389/fgene.2015.00208)

### 3.1 Abstract

To gain a detailed understanding of how plant microbes evolve and adapt to hosts, pesticides, and other factors, knowledge of the population dynamics and evolutionary history of populations is crucial. Plant pathogen populations are often clonal or partially clonal which requires different analytical tools. With the advent of high throughput sequencing technologies, obtaining genome-wide population genetic data has become easier than ever before. We previously contributed the R package *poppr* specifically addressing issues with analysis of clonal populations. In this paper we provide several significant extensions to *poppr* with a focus on large, genome-wide SNP data. Specifically, we provide several new functionalities including the new function `mlg.filter` to define clone boundaries allowing for inspection and definition of what is a clonal lineage, minimum spanning networks with reticulation, a sliding-window analysis of the index of association, modular bootstrapping of any genetic distance, and analyses across any level of hierarchies.

### 3.2 Introduction

To paraphrase Dobzhansky, nothing in the field of plant-microbe interactions makes sense except in the light of population genetics (Dobzhansky, 1973). Genetic forces such as selection and drift act on alleles in a population. Thus, a true understanding of how plant pathogens emerge, evolve and adapt to crops, fungicides, or other factors, can only be elucidated in the context of population level phenomena given the demographic history of populations (Grünwald and Goss, 2011; McDonald and Linde, 2002;

Milgroom et al., 1989). The field of population genetics, in the era of whole genome resequencing, provides unprecedented power to describe the evolutionary history and population processes that drive coevolution between pathogens and hosts. This powerful field thus critically enables effective deployment of R genes, design of pathogen informed plant resistance breeding programs, and implementation of fungicide rotations that minimize emergence of resistance.

Most computational tools for population genetics are based on concepts developed for sexual model organisms. Populations that reproduce clonally or are polyploid are thus difficult to characterize using classical population genetic tools because theoretical assumptions underlying the theory are violated. Yet, many plant pathogen populations are at least partially clonal if not completely clonal (Anderson and Kohn, 1995; Milgroom, 1996). Thus, development of tools for analysis of clonal or polyploid populations is needed.

Genotyping by sequencing and whole genome resequencing provide the unprecedented ability to identify thousands of single nucleotide polymorphisms (SNPs) in populations (Davey et al., 2011; Elshire et al., 2011; Luikart et al., 2003). With traditional marker data (e.g., SSR, AFLP) a clone was typically defined as a unique multilocus genotype (MLG) (Cooke et al., 2012; Falush et al., 2003; Goss et al., 2009; Grünwald and Hoheisel, 2006; Taylor and Fisher, 2003). Availability of large SNP data sets provides new challenges for data analysis. These data are based on reduced representation libraries and high throughput sequencing with moderate sequencing depth which invariably results in substantial missing data, error in SNP calling due to sequencing error, lack of read depth or other sources of spurious allele calls (Mastretta-Yanes et

al., 2014). It is thus not clear what a clone is in large SNP data sets and novel tools are required for definition of clone boundaries.

The research community using the R statistical and computing language (R Core Team, 2015) has developed a plethora of new resources for population genetic analysis. R is particularly appealing because all code is open source and functions can be evaluated and modified by any user. Recently, we introduced the R package *poppr* specifically developed for analysis of clonal populations (Kamvar et al., 2014b). *Poppr* previously introduced several novel features including the ability to conduct a hierarchical analysis across unlimited hierarchies, test for linkage association, graph minimum spanning networks or provide bootstrap support for Bruvo's distance in resulting trees. *Poppr* has been rapidly adopted and applied to a range of studies including for example horizontal transmission in leukemia of clams (Metzger et al., 2015), study of the vector-mediated parent-to-offspring transmission in an avian malaria-like parasite (Chakarov et al., 2015), and characterization of the emergence of the invasive forest pathogen *Hymenoscyphus pseudoalbidus* (Gross et al., 2014). It has also been used to implement real-time, online R based tools for visualizing relationships among unknown MLGs in reference databases ([\(http://phytophthora-id.org/\)](http://phytophthora-id.org/)) (Grünwald et al., 2011).

Here, we introduce *poppr* 2.0, which provides a major update to *poppr* (Kamvar et al., 2014b) including novel tools for analysis of clonal populations specifically addressing large SNP data. Significant novel tools include functions for calculating clone boundaries and collapsing individuals into clonal groups based on a user-specified genetic distance threshold, sliding window analyses, genotype accumulation curves, reticula-

tions in minimum spanning networks, and bootstrapping for any genetic distance.

### 3.3 Implementations and Examples

#### 3.3.1 Clonal identification

As highlighted in previous work, clone correction is an important component of population genetic analysis of organisms that are known to reproduce asexually (Grünwald et al., 2003; Kamvar et al., 2014b; Milgroom, 1996). This method is a partial correction for bias that affects metrics that rely on allele frequencies assuming panmixia and was initially designed for data with only a handful of markers. With the advent of large-scale sequencing and reduced-representation libraries, it has become easier to sequence tens of thousands of markers from hundreds of individuals (Davey and Blaxter, 2010; Davey et al., 2011; Elshire et al., 2011). With this larger number of markers, the genetic resolution is much greater, but the chance of genotyping error is also greatly increased and missing data is frequent (Mastretta-Yanes et al., 2014). Taking this fact and occasional somatic mutations into account, it would be impossible to separate true clones from independent individuals by just comparing what MLGs are different. We introduce a new method for collapsing unique multilocus genotypes determined by naive string comparison into multilocus lineages utilizing any genetic distance given three different clustering algorithms: farthest neighbor, nearest neighbor, and UPGMA (average neighbor) (Sokal, 1958).

These clustering algorithms act on a distance matrix that is either provided by the

user or generated via a function that will calculate a distance from genetic data such as `bruvo.dist`, which in particular applies to any level of ploidy (Bruvo et al., 2004). All algorithms have been implemented in C and utilize the OpenMP framework for optional parallel processing (Dagum and Menon, 1998). Default is the conservative farthest neighbor algorithm (Fig. 3.1A), which will only cluster samples together if all samples in the cluster are at a distance less than the given threshold. By contrast, the nearest neighbor algorithm will have a chaining effect that will cluster samples akin to adding links on a chain where a sample can be included in a cluster if all of the samples have at least one connection below a given threshold (Fig. 3.1C). The UPGMA, or average neighbor clustering algorithm is the one most familiar to biologists as it is often used to generate ultra-metric trees based on genetic distance (Fig. 3.1B). This algorithm will cluster by creating a representative sample per cluster and joining clusters if these representative samples are closer than the given threshold.

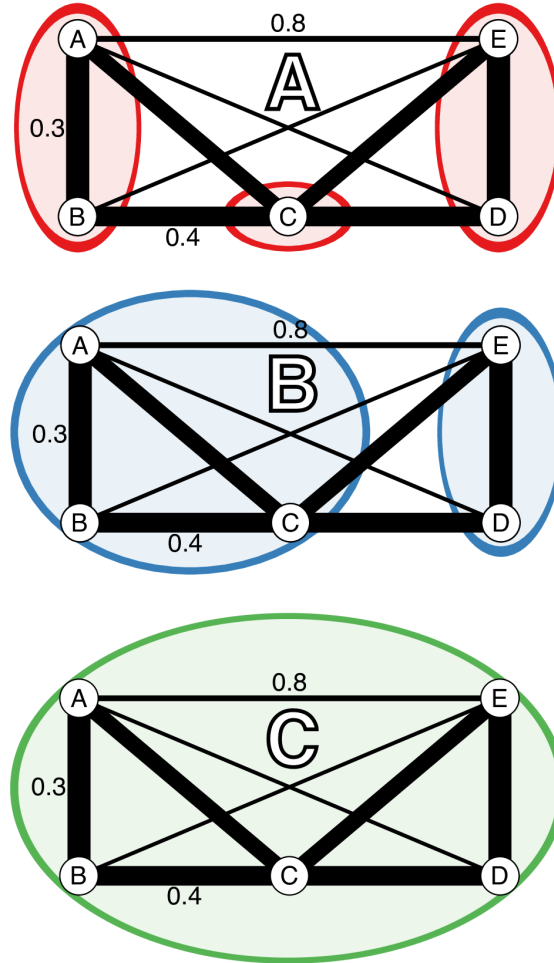


Figure 3.1: Diagrammatic representation of the three clustering algorithms implemented in `mlg.filter`. **(A-C)** Represent different clustering algorithms on the same imaginary network with a threshold of 0.451. Edge weights are represented in arbitrary units noted by the line thickness and numerical values next to the lines. All outer angles are 90 degrees, so the un-labeled edge weights can be obtained with simply geometry. Colored circles represent clusters of genotypes. **(A)** Farthest neighbor clustering does not cluster nodes B and C because nodes A and C are more than a distance of 0.451 apart. **(B)** UPGMA (average neighbor) clustering clusters nodes A, B, and C together because the average distance between them and C is  $< 0.451$ . **(C)** Nearest neighbor clustering clusters all nodes together because the minimum distance between them is always  $< 0.451$ .

We utilize data from the microbe *Phytophthora infestans* to show how the `mlg.filter` function collapses multilocus genotypes with Bruvo's distance assuming a genome addition model (Bruvo et al., 2004). *P. infestans* is the causal agent of potato late blight originating from Mexico that spread to Europe in the mid 19th century (Goss et al., 2014; Yoshida et al., 2013). *P. infestans* reproduces both clonally and sexually. The clonal lineages of *P. infestans* have been formally defined into 18 separate clonal lineages using a combination of various molecular methods including AFLP and microsatellite markers (Lees et al., 2006; Li et al., 2013). For these data, we used `mlg.filter` to detect all of the distance thresholds at which 18 multilocus lineages would be resolved. We used these thresholds to define multilocus lineages and create contingency tables and dendograms to determine how well the multilocus lineages were detected.

For the *P. infestans* population, the three algorithms were able to detect 18 multilocus lineages at different distance thresholds (Fig. 3.2). Contingency tables between the described multilocus genotypes and the genotypes defined by distance show that most of the 18 lineages were resolved, except for US-8, which is polytomic (Table 3.1).

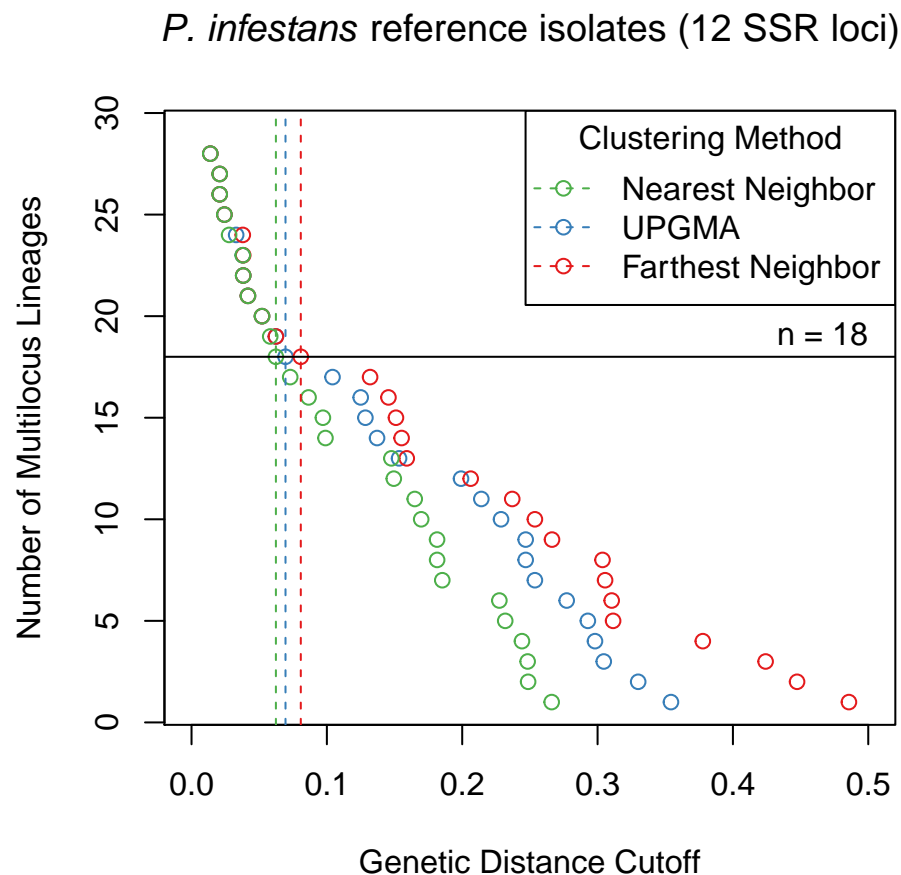


Figure 3.2: Graphical representation of three different clustering algorithms collapsing multilocus genotypes for 12 SSR loci from *Phytophthora infestans* representing 18 clonal lineages. The horizontal axis is Bruvo's genetic distance assuming the genome addition model. The vertical axis represents the number of multilocus lineages observed. Each point shows the threshold at which one would observe a given number of multilocus genotypes. The horizontal black line represents 18 multilocus genotypes and vertical dashed lines mark the thresholds used to collapse the multilocus genotypes into 18 multilocus lineages.

	3	4	5	6	8	10	12	15	16	17	18	20	21	22	24	25	27	28
B	.	.	.	.	.	.	.	.	.	.	.	.	.	.	.	.	.	.
C	.	.	.	.	.	.	.	.	.	.	.	.	.	.	.	.	.	.
D.1	.	.	.	.	.	.	.	.	.	.	.	.	.	.	.	.	.	.
D.2	.	.	.	.	.	.	.	.	.	.	.	.	.	.	.	.	.	.
EU-13	.	.	.	.	.	.	.	.	1	.	.	.	.	.	.	.	.	.
EU-4	.	.	.	.	.	.	.	.	.	1	.	.	.	.	.	.	.	.
EU-5	.	.	.	.	.	.	.	.	.	.	2	.	.	.	.	.	.	.
EU-8	.	.	.	.	.	.	.	.	1	.	.	.	.	.	.	.	.	.
US-11	.	.	.	.	.	.	.	.	.	.	.	.	.	.	.	.	2	.
US-12	.	1	.	.	.	.	.	.	.	.	.	.	.	.	.	.	.	.
US-14	.	.	.	.	.	.	.	.	1	.	.	.	.	.	.	.	.	.
US-17	.	.	.	.	.	.	.	.	.	.	.	.	1	.	.	.	.	.
US-20	2	.	.	.	.	.	.	.	.	.	.	.	.	.	.	.	.	.
US-21	.	.	.	.	.	.	.	.	.	.	.	.	.	.	.	.	.	2
US-22	.	.	.	.	.	.	.	.	.	.	.	.	.	2	.	.	.	.
US-23	.	.	.	.	.	.	.	.	.	3	.	.	.	.	.	.	.	.
US-24	.	.	.	.	3	.	.	.	.	.	.	.	.	.	.	.	.	.
US-8	.	1	1	.	2	.	.	.	.	.	.	.	.	.	.	.	.	.

Table 3.1: Contingency table comparing multilocus lineages (MLL) defined in Li et al. (2013) and Lees et al. (2006) (rows) to MLLs inferred from Bruvo's genetic distance (columns) at a threshold of 0.07 with the average neighbor algorithm (Bruvo et al., 2004; Sokal, 1958). Values in the table represent the number of times any given inferred MLL matches with a previously defined MLL. For example, in our original data set, there were three genotypes previously defined as the US-24 MLL. All three genotypes were also determined to cluster into a single MLL by filtering. In contrast, US-8 was determined to cluster into three different MLLs by filtering.

We utilized simulated data to evaluate the effect of sequencing error and missing data on MLG calling. We constructed the data using the `glSim` function in *adegenet* (Jombart and Ahmed, 2011) to obtain a SNP data set for demonstration. Two diploid data sets were created, each with 10k SNPs (25% structured into two groups) and 200 samples with 10 ancestral populations of even sizes. Clones were created in one data set by marking each sample with a unique identifier and then randomly sampling with replacement. It is well documented that reduced- representation sequencing can introduce several erroneous calls and missing data (Mastretta-Yanes et al., 2014). To reflect this, we mutated SNPs at a rate of 10% and inserted an average of 10% missing data for each sample after clones were created, ensuring that no two sequences were alike. The number of mutations and missing data per sample were determined by sampling from a Poisson distribution with  $\lambda = 1000$ . After pooling, 20% of the data set was randomly sampled for analysis. Genetic distance was obtained with the function `bitwise.dist`, which calculates the fraction of different sites between samples equivalent to Provesti's distance, counting missing data as equivalent in comparison (Prevosti et al., 1975).

All three filtering algorithms were run with a threshold of 1, returning a numeric vector of length  $n - 1$  where each element represented a threshold at which two samples/clusters would join. Since each data set would have varying distances between samples, the clonal boundary threshold was defined as the midpoint of the largest gap between two thresholds that collapsed less than 50% of the data.

Out of the 100 simulations run, we found that across all methods, detection of duplicated samples had  $\sim 98\%$  true positive fraction and  $\sim 0.8\%$  false positive frac-

tion indicating that this method is robust to simulated populations (supplementary materials<sup>1</sup>).

### 3.3.2 Minimum Spanning Networks with Reticulation

In its original iteration, *poppr* introduced minimum spanning networks that were based on the *igraph* function `minimum.spanning.tree` (Csardi and Nepusz, 2006). This algorithm produces a minimum spanning tree with no reticulations where nodes represent individual MLGs. In other minimum spanning network programs, reticulation is obtained by calculating the minimum spanning tree several times and returning the set of all edges included in the trees. Due to the way *igraph* has implemented Prim's algorithm, it is not possible to utilize this strategy, thus we implemented an internal C function to walk the space of minimum spanning trees based on genetic distance to connect groups of nodes with edges of equal weight.

To demonstrate the utility of minimum spanning networks with reticulation, we used two clonal data sets: the H3N2 flu virus data from the *adegenet* package using years of each epidemic as the population factor, and *Phytophthora ramorum* data from Nurseries and Oregon forests (Jombart et al., 2010; Kamvar et al., 2014a). Minimum spanning networks were created with and without reticulation using the *poppr* functions `diss.dist` and `bruvo.msn` for the H3N2 and *P. ramorum* data, respectively (Bruvo et al., 2004; Kamvar et al., 2014b). To detect mlg clusters, the infoMAP community detection algorithm was applied with 10,000 trials as implemented in the R package

---

<sup>1</sup>Supplementary data available at <https://github.com/grunwaldlab/supplementary-poppr-2.0>; DOI: [10.5281/zenodo.17424](https://doi.org/10.5281/zenodo.17424)

*igraph* version 0.7.1 utilizing genetic distance as edge weights and number of samples in each MLG as vertex weights (Csardi and Nepusz, 2006; Rosvall and Bergstrom, 2008).

To evaluate the results, we compared the number, size, and entropy ( $H$ ) of the resulting communities as we expect a highly clonal organism with low genetic diversity to result in a few, large communities. We also created contingency tables of the community assignments with the defined populations and used those to calculate entropy using Shannon's index with the function *diversity* from the R package *vegan* version 2.2-1 (Oksanen et al., 2015; Shannon, 2001). A low entropy indicates presence of a few large communities whereas high entropy indicates presence of many small communities.

The infoMAP algorithm revealed 63 communities with a maximum community size of 77 and  $H = 3.56$  for the reticulate network of the H3N2 data and 117 communities with a maximum community size of 26 and  $H = 4.65$  for the minimum spanning tree. The entropy across years was greatly decreased for all populations with the reticulate network compared to the minimum spanning tree (Fig. 3.3). Note that the reticulated network (Fig. 3.3B) showed patterns corresponding with those resulting from a discriminant analysis of principal components (Fig. 3.3D) (Jombart et al., 2010).

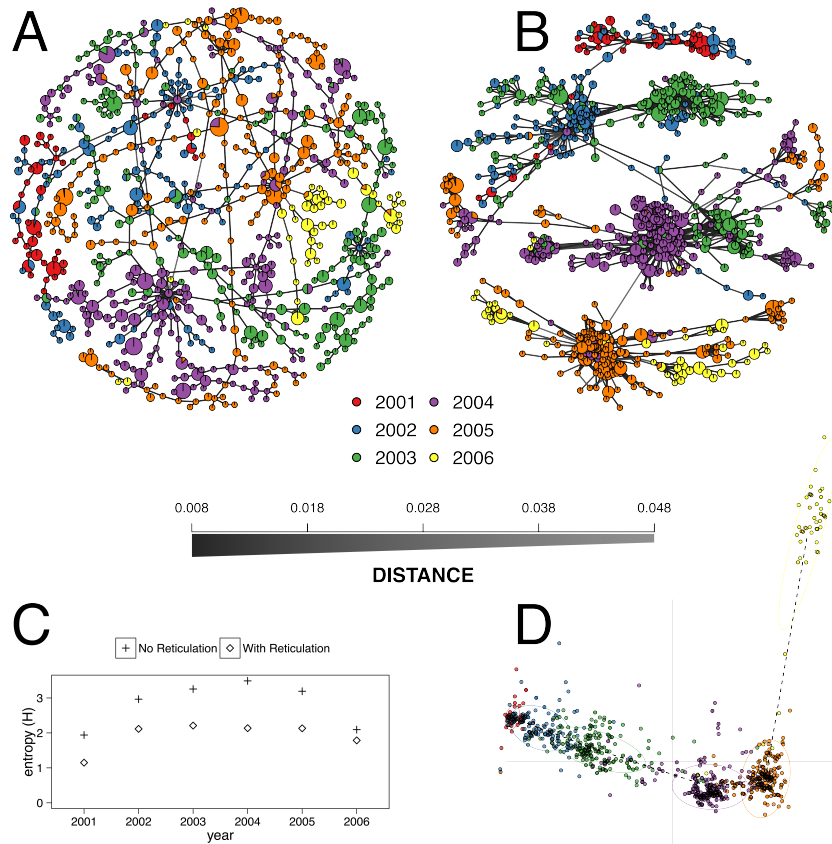


Figure 3.3: **(A-B)** Minimum spanning networks of the hemagglutinin (HA) segment of H3N2 viral DNA from the *adegenet* package representing flu epidemics from 2001 to 2006 without reticulation **(A)** and with reticulation **(B)** (Jombart, 2008; Jombart et al., 2010). Each node represents a unique multilocus genotype, colors represent epidemic year, and edge color represents absolute genetic distance. **(C)** Shannon entropy values for population assignments compared with communities determined by the infoMAP algorithm on **(A)** and **(B)**. **(D)** Graphic reproduced from Jombart et al. (2010) showing that the 2006 epidemic does not cluster neatly with the other years via Discriminant Analysis of Principal Components. Horizontal axis represents the first discriminant component. Vertical axis represents the second discriminant component.

Graph walking of the reticulated minimum spanning network of *P. ramorum* by the infoMAP algorithm revealed 16 communities with a maximum community size of 13 and  $H = 2.60$ . The un-reticulated minimum spanning tree revealed 20 communities with a maximum community size of 7 and  $H = 2.96$ . In the ability to predict Hunter Creek as belonging to a single community, the reticulated network was successful whereas the minimum spanning tree separated one genotype from that community. The entropy for the reticulated network was lower for all populations except for the coast population (supplementary materials<sup>2</sup>).

### 3.3.3 Bootstrapping

Assessing population differentiation through methods such as  $G_{st}$ , AMOVA, and Mantel tests relies on comparing samples within and across populations (Excoffier et al., 1992; Mantel, 1967; Nei, 1973). Confidence in distance metrics is related to the confidence in the markers to accurately represent the diversity of the data. Especially true with microsatellite markers, a single hyper-diverse locus can make a population appear to have more diversity based on genetic distance. Using a bootstrapping procedure of randomly sampling loci with replacement when calculating a distance matrix provides support for clades in hierarchical clustering.

Data in genind and genpop objects are represented as matrices with individuals in rows and alleles in columns (Jombart, 2008). This gives the advantage of being able to use R's matrix algebra capabilities to efficiently calculate genetic distance.

---

<sup>2</sup>Supplementary data available at <https://github.com/grunwaldlab/supplementary-poppr-2.0>; DOI: [10.5281/zenodo.17424](https://doi.org/10.5281/zenodo.17424)

Unfortunately, this also means that bootstrapping is a non-trivial task as all alleles at a single locus need to be sampled together. To remedy this, we have created an internal S4 class called “bootgen”, which extends the internal “gen” class from *adegenet*. This class can be created from any genind, genclose, or genpop object, and allows loci to be sampled with replacement. To further facilitate bootstrapping, a function called *aboot*, which stands for “any boot”, is introduced that will bootstrap any genclose, genind, or genpop object with any genetic distance that can be calculated from it.

To demonstrate calculating a dendrogram with bootstrap support, we used the *poppr* function *aboot* on population allelic frequencies derived from the data set *microbov* in the *adegenet* package with 1000 bootstrap replicates (Jombart, 2008; Laloë et al., 2007). The resulting dendrogram shows bootstrap support values > 50% (Fig. 3.4) and used the following code:

```
library("poppr");

data("microbov", package = "adegenet");

strata(microbov) <- data.frame(other(microbov));

setPop(microbov) <- ~coun/spe/breed;

bov_pop <- genind2genpop(microbov);

set.seed(20150428);

pop_tree <- aboot(bov_pop, sample = 1000, cutoff = 50);
```

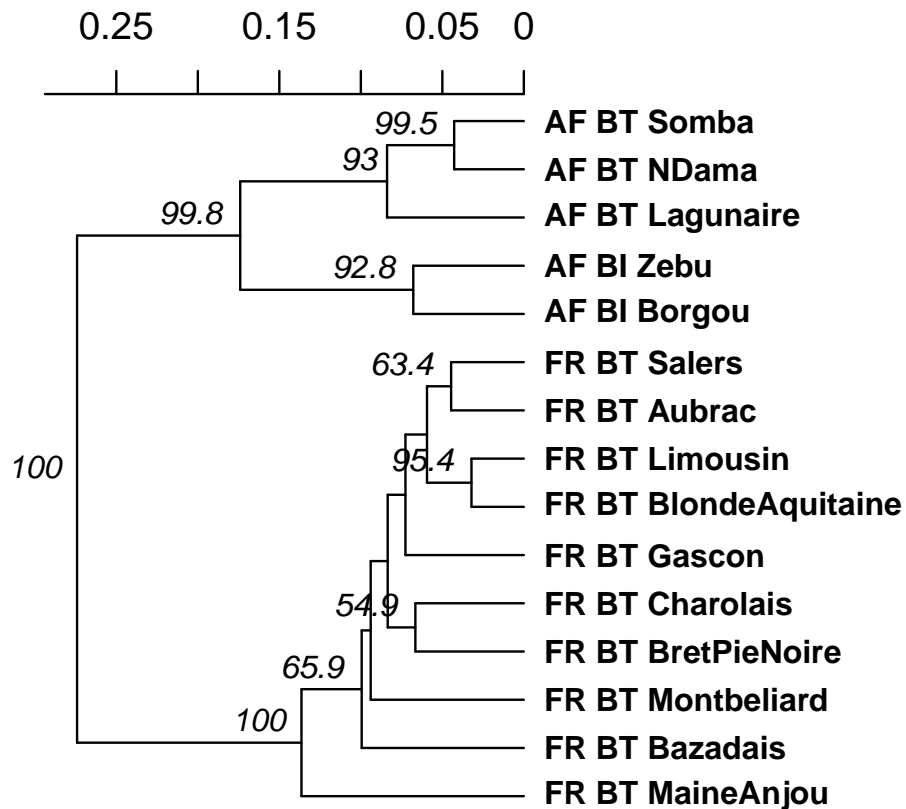


Figure 3.4: UPGMA dendrogram generated from Nei's genetic distance on 15 breeds of *Bos taurus* (BT) or *Bos indicus* (BI) from Africa (AF) or France (FR). These data are from Laloë et al. (2007). Node labels represent bootstrap support > 50% out of 1,000 bootstrap replicates.

### 3.3.4 Genotype Accumulation Curve

Analysis of population genetics of clonal organisms often borrows from ecological methods such as analysis of diversity within populations (Arnaud-Hanod et al., 2007; Grünwald et al., 2003; Milgroom, 1996). When choosing markers for analysis, it is important to make sure that the observed diversity in your sample will not appreciably increase if

an additional marker is added (Arnaud-Hanod et al., 2007). This concept is analogous to a species accumulation curve, obtained by rarefaction. The genotype accumulation curve in *poppr* is implemented in the function `genotype_curve`. The curve is constructed by randomly sampling  $x$  loci and counting the number of observed MLGs. This repeated  $r$  times for 1 locus up to  $n - 1$  loci, creating  $n - 1$  distributions of observed MLGs.

The following code example demonstrates the genotype accumulation curve for data from Everhart and Scherm (2015) showing that these data reach a small plateau and have a greatly decreased variance with 12 markers, indicating that there are enough markers such that adding more markers to the analysis will not create very many new genotypes (Fig. 3.5).

```
library("poppr");
library("ggplot2");
data("monpop", package = "poppr");

set.seed(20150428);

genotype_curve(monpop, sample = 1000);
p <- last_plot() + theme_bw();    # get the last plot
p + geom_smooth(aes(group = 1)); # plot with a trendline
```

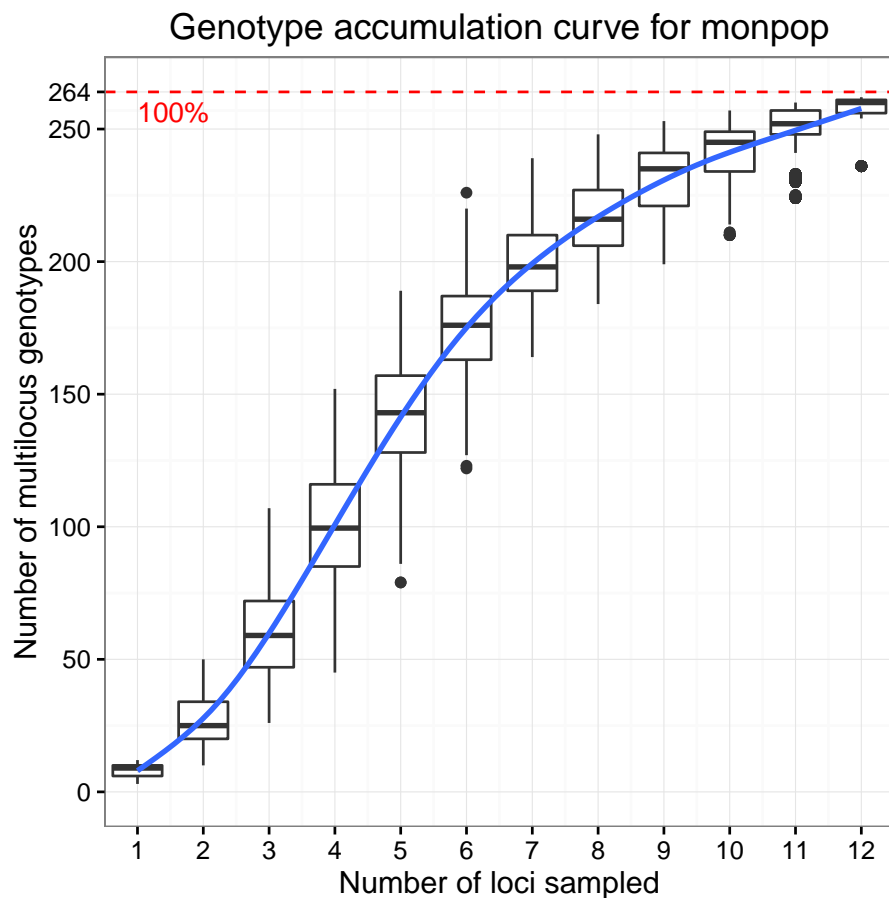


Figure 3.5: Genotype accumulation curve for 694 isolates of the peach brown rot pathogen, *Monilinia fructicola* genotyped over 13 loci from Everhart and Scherm (2015). The horizontal axis represents the number of loci randomly sampled without replacement up to  $n - 1$  loci, the vertical axis shows the number of multilocus genotypes observed, up to 262, the number of unique multilocus genotypes in the data set. The red dashed line represents 90% of the total observed multilocus genotypes. A trendline (blue) has been added using the `ggplot2` function `stat_smooth`.

### 3.3.5 Index of association

The index of association ( $I_A$ ) is a measure of multilocus linkage disequilibrium that is most often used to detect clonal reproduction within organisms that have the ability to reproduce via sexual or asexual processes (Brown et al., 1980; Milgroom, 1996; Smith et al., 1993). It was standardized in 2001 as  $\bar{r}_d$  by Agapow and Burt (2001) to address the issue of scaling with increasing number of loci. This metric is typically applied to traditional dominant and co-dominant markers such as AFLPs, SNPs, or microsatellite markers. With the advent of high throughput sequencing, SNP data is now available in a genome-wide context and in very large matrices including thousands of SNPs. For this reason, we devised two approaches using the index of association for large numbers of markers typical for population genomic studies. Both functions utilize *adegenet*'s “genlight” object class, which efficiently stores 8 binary alleles in a single byte (Jombart and Ahmed, 2011). As calculation of the  $\bar{r}_d$  requires distance matrices of absolute number of differences, we utilize a function that calculates these distances directly from the compressed data called `bitwise.dist`.

The first approach is a sliding window analysis implemented in the function `win.ia`. It utilizes the position of markers in the genome to calculate  $\bar{r}_d$  among any number of SNPs found within a user-specified windowed region. It is important that this calculation utilize  $\bar{r}_d$  as the number of loci will be different within each window (Agapow and Burt, 2001). This approach would be suited for a quick calculation of linkage disequilibrium across the genome that can detect potential hotspots of LD that could be investigated further with more computationally intensive methods assuming that

the number of samples << the number of loci.

As it would necessarily focus on loci within a short section of the genome that may or may not be recombining, a sliding window approach would not be good for utilizing  $\bar{r}_d$  as a test for clonal reproduction. A remedy for this is implemented in the function `samp.ia`, which will randomly sample  $m$  loci, calculate  $\bar{r}_d$ , and repeat  $r$  times, thus creating a distribution of expected values of  $\bar{r}_d$ .

To demonstrate the sliding window and random sampling of  $\bar{r}_d$  with respect to clonal populations, we simulated two populations containing 1,100 neutral SNPs for 100 diploid individuals under the same initial seed. One population had individuals randomly sampled with replacement, representing the clonal population. After sampling, both populations had 5% random error and 1% missing data independently propagated across all samples. On average, we obtained a higher value of  $\bar{r}_d$  for the clonal population compared to the sexual population for both methods (Fig. 3.6).

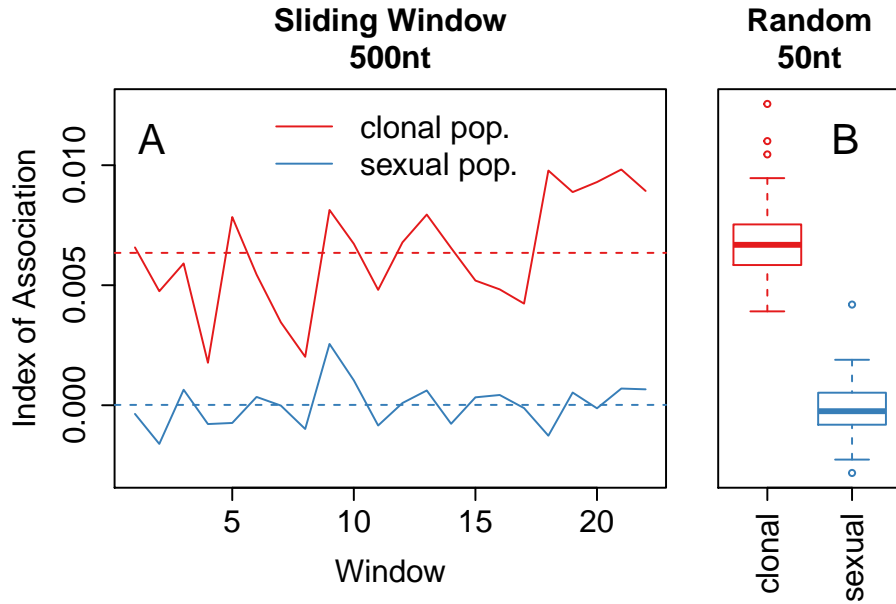


Figure 3.6: **(A)** Sliding window analysis of the standardized index of association ( $\bar{r}_d$ ) across a simulated  $1.1 \times 10^4$  nt chromosome containing 1,100 variants among 100 individuals. Each window analyzed variants within 500nt chunks. The black line refers to the clonal and the blue line to the sexual populations. **(B)** boxplots showing 100 random samples of 50 variants to calculate a distribution of  $\bar{r}_d$  for the clonal (red) and sexual (blue) populations. Each box is centered around the mean, with whiskers extending out to 1.5 times the interquartile range. The median is indicated by the center line. **(A)** and **(B)** are plotted on the same y-axis.

### 3.3.6 Data format updates: population strata and hierarchies

Assessments of population structure through methods such as hierarchical  $F_{st}$  (Goudet, 2005) and AMOVA (Michalakis and Excoffier, 1996) require hierarchical sampling of populations across space or time (Everhart and Scherm, 2015; Grünwald and Hoheisel, 2006; Linde et al., 2002). With clonal organisms, basic practice has been to clone-

censor data to avoid downward bias in diversity due to duplicated genotypes that may or may not represent different samples (Milgroom, 1996). This correction should be performed with respect to a population hierarchy to accurately reflect the biology of the organism. Traditional data structures for population genetic data in most analysis tools allow for only one level of hierarchical definition. The investigator thus had to provide the data set for analysis at each hierarchical level.

To facilitate handling hierarchical and multilocus genotypic metadata, *poppr* version 1.1 introduced a new S4 data object called “genclone”, extending *adegenet*’s “genind” object (Kamvar and Grünwald, unpublished). The genclone object formalized the definitions of multilocus genotypes and population hierarchies by adding two slots called “mlg” and “hierarchy” that carried a numeric vector and a data frame, respectively. These new slots allow for increased efficiency and ease of use by allowing these metadata to travel with the genetic data. The hierarchy slot in particular contains a data frame where each column represents a separate hierarchical level. This is then used to set the population factor of the data by supplying a hierarchical formula containing one or more column names of the data frame in the hierarchy slot.

The functionality represented by the hierarchy slot has now been migrated from the *poppr* to the *adegenet* package version 2.0 to allow hierarchical analysis in *adegenet*, *poppr*, and other dependent packages. The prior *poppr* hierarchy slot and methods have now been renamed strata in *adegenet*. A short example of the utility of these methods can be seen in the code segment under **Bootstrapping**, above. This migration provides end users with a broader ability to analyze data hierarchically in R across packages.

## 3.4 Availability

As of this writing, the *poppr* R package version 2.0 containing all of the features described here is located at <https://github.com/grunwaldlab/poppr/tree/2.0-rc>. It is necessary to install *adegenet* 2.0 before installing *poppr*. It can be found at <https://github.com/thibautjombart/adegenet>. Both of these can be installed via the R package *devtools* (Wickham and Chang, 2015). More information and example code can be found in the supplementary materials<sup>3</sup>.

### 3.4.1 Requirements

- R version 3.0 or better
- A C compiler. For windows, it can be obtained via Rtools (<http://cran.r-project.org/bin/windows/Rtools/>). On OSX, it can be obtained via Xcode.

For parallel support, gcc version 4.6 or better is needed.

---

<sup>3</sup>Supplementary data available at <https://github.com/grunwaldlab/supplementary-poppr-2.0>; DOI: [10.5281/zenodo.17424](https://doi.org/10.5281/zenodo.17424)

### 3.4.2 Installation

From within R, *poppr* can be installed via:

```
install.packages("devtools")
library("devtools")
install_github("thibautjombart/aegenet")
install_github("grunwaldlab/poppr@2.0-rc")
```

Several population genetics packages in R are currently going through a major upgrade following the 2015 R hackathon on population genetics (<https://github.com/NESCent/r-popgen-hackathon>) and have not yet been updated in CRAN. We will upload *poppr* 2.0 to CRAN once all other reverse dependent packages have been updated.

## 3.5 Discussion

Given low cost and high throughput of current sequencing technologies we are entering a new era of population genetics where large SNP data sets with thousands of markers are becoming available for large populations in a genome-wide context. This data provides new possibilities and challenges for population genetic analyses. We provide novel tools that enable analysis of this data in R with a particular emphasis on clonal organisms.

Particularly useful is the implementation of  $\bar{r}_d$  in a genomic context (Agapow and Burt, 2001). Random sampling of loci across the genome can give an expected distri-

bution of  $\bar{r}_d$ , which is expected to have a mean of zero for panmictic populations. This metric is not affected by the number of loci sampled, is model free, and has the ability to detect population structure.  $\bar{r}_d$  is also implemented for sliding window analyses that are useful to detect candidate regions of linkage disequilibrium for further analysis.

Clustering multilocus genotypes into multilocus lineages based on genetic distances is a non-trivial task given large SNP data sets. Moreover, this has not previously been implemented for genomic data for clonal populations. Clonal assignment has previously been available in the programs GENCLONE and GENODIVE for classical markers (Arnaud-Hanod et al., 2007; Meirmans and Van Tienderen, 2004). Our method with `mlg.filter` builds upon this idea and allows the user to choose between three different approaches for clustering MLGs. The choice of clustering algorithm has an impact on the data (Fig. 3.1, 3.2), where for example a genetic distance cutoff of 0.1 would be the difference between 14 multilocus lineages (MLLs) and 17 MLLs for nearest neighbor and UPGMA clustering, respectively (Fig. 3.2). The option to choose the clustering algorithm gives the user the ability to choose what is biologically relevant to their populations. While there is not one optimal procedure for defining boundaries in clonal lineages, our tool provides a means of exploring the potential MLG or MLL boundary space.

Minimum spanning networks are a useful tool to analyze the relationships between individuals in a population, because it reduces the complexity of a distance matrix to the connections that are strongest. By default, these networks are drawn without reticulations, but for clonal organisms where many of the connections between samples are equivalent, the minimum spanning network appears as a chain and reduces the

information that can be communicated. This is problematic because the ability to detect population structure with one instance of a minimum spanning network is limited. Adding reticulation into the minimum spanning network thus presents all equivalent connections and allows population structure to be more readily detectable. As shown in Fig. 3.3, population structure is apparent both visually and by graph community detection algorithms such as the infoMAP algorithm (Rosvall and Bergstrom, 2008). Additionally, the current implementation in *poppr* has been successfully used in analyses such as reconstruction of the *P. ramorum* epidemic in Oregon forests (Kamvar et al., 2014a, 2015c).

*Poppr* 2.0 is open source and available on GitHub. Members of the community are invited to contribute by raising issues or pull requests on our repository at <https://github.com/grunwaldlab/poppr/issues>.

### 3.6 Acknowledgements

We thank Ignazio Carbone for discussions on the index of association; David Cooke, Sanmohan Baby, and Jens Hansen for beta testing; and Thibaut Jombart for allowing us to incorporate the `strata` slot and related methods in `adegenet`. We also thank all the members of the 2015 R hackathon on population genetics in Durham, NC for their advice and input (<https://github.com/NESCent/r-popgen-hackathon>). This work was supported in part by US Department of Agriculture (USDA) Agricultural Research Service Grant 5358-22000-039-00D, USDA National Institute of Food and Agriculture Grant 2011-68004-30154, USDA APHIS, the USDA-ARS Floriculture Nursery Initiative, and the USDA-Forest Service Forest Health Monitoring Program (to NJG).

## Chapter 4: Spatial and Temporal Analysis of Populations of the Sudden Oak Death Pathogen in Oregon Forests

Zhian N. Kamvar, Meredith M. Larsen, Alan M. Kanaskie, Everett M. Hansen, and  
Niklaus J. Grünwald

Journal: **Phytopathology**  
3340 Pilot Knob Rd, St Paul, MN 55121, USA  
Published 2015-07, Volume 105, Issue: 7, DOI: [10.1094/PHYTO-12-14-0350-FI](https://doi.org/10.1094/PHYTO-12-14-0350-FI)

#### 4.1 Abstract

Sudden oak death caused by the oomycete *Phytophthora ramorum* was first discovered in California toward the end of the 20th century and subsequently emerged on tanoak forests in Oregon before its first detection in 2001 by aerial surveys. The Oregon Department of Forestry has since monitored the epidemic and sampled symptomatic tanoak trees from 2001 to the present. Populations sampled over this period were genotyped using microsatellites and studied to infer the population genetic history. To date, only the NA1 clonal lineage is established in this region, although three lineages exist on the North American west coast. The original introduction into the Joe Hall area eventually spread to several regions: mostly north but also east and southwest. A new introduction into Hunter Creek appears to correspond to a second introduction not clustering with the early introduction. Our data are best explained by both introductions originating from nursery populations in California or Oregon and resulting from two distinct introduction events. Continued vigilance and eradication of nursery populations of *P. ramorum* are important to avoid further emergence and potential introduction of other clonal lineages.

#### 4.2 Introduction

Sudden oak death (SOD) emerged as a severe epidemic disease on coast live oak (*Quercus agrifolia*) and tanoak (*Notholithocarpus densiflorus*) in California in the mid 1990s and reemerged shortly thereafter on tanoak in Oregon in the early 2000s (Everhart et al., 2014; Grünwald et al., 2008a; Hansen et al., 2008; Rizzo et al., 2005).

SOD is caused by *Phytophthora ramorum* Werres, De Cock & Man in't Veld, and is considered to be one of the top two oomycete pathogens based on its scientific and economic importance (Kamoun et al., 2014; Werres et al., 2001). The Oregon epidemic was first detected during aerial surveys in 2001 on tanoak but likely derived from initial introductions in the late 1990s. The Oregon Department of Forestry has since monitored the epidemic and sampled symptomatic tanoaks since 2001 (Hansen et al., 2008). Strains sampled from infected sites in forest or nursery environments have been genotyped in several labs using a range of microsatellite loci (Grünwald et al., 2009; Ivors et al., 2006; Prospero et al., 2004, 2009, 2007).

*P. ramorum* has emerged repeatedly around the world as 4 distinct clonal lineages found in North America (lineages NA1, NA2, and EU1) and Europe (EU1 and EU2) (Grünwald et al., 2012; Ivors et al., 2006; Poucke et al., 2012). The lineages have been named by the continent on which they first appeared, i.e. North America (= NA) or Europe (= EU) and are numbered in order of discovery (Grünwald et al., 2009). The NA1 clonal lineage was first discovered in California causing SOD on tanoak and coast live oak and is the one currently found in Curry County, Oregon, USA (Mascheretti et al., 2008). The EU1 and NA2 populations were discovered later in nursery environments and are currently only found in California, Oregon, Washington and British Columbia while the NA1 clone has been shipped with nursery plants from the West to the Southern and Southwestern US (Goss et al., 2009, 2011; Grünwald et al., 2012; Ivors et al., 2006; Mascheretti et al., 2008; Prospero et al., 2009). The EU1 clonal lineage is the one first discovered in Europe, but in 2007 the new EU2 lineage emerged in Northern Ireland and since migrated to Western Scotland (Poucke

et al., 2012; Werres et al., 2001). EU1 was first introduced to Europe and eventually migrated to the Pacific Northwest of North America (Goss et al., 2011).

*P. ramorum* populations sampled in Oregon forests to date belong exclusively to the NA1 clonal lineage (Hansen et al., 2008; Prospero et al., 2007). Given that NA2 and/or EU1 clones have been found in California, Oregon, Washington, and/or British Columbia in association with nursery plant movements, introduction of NA2 or EU1 from nursery environments to Curry County forests is a plausible scenario (Goss et al., 2009, 2011; Grünwald et al., 2012; Prospero et al., 2009, 2007). Our present work thus monitors populations and potential emergence of novel lineages in Oregon forests.

Our main objectives here are to describe the spatial and temporal pattern of the populations and clonal dynamic of the SOD pathogen in Curry County in southwestern Oregon from 2001 to the present. Specifically, we asked (1) if novel lineages have been introduced into the forests in Curry County, (2) if multiple introductions occurred, and (3) whether introduction might have come from nursery populations. We sampled infected tanoaks between 2001-2014 and characterized populations using microsatellite analysis.

## 4.3 Materials and Methods

### 4.3.1 Location

The SOD infested areas are located in the Siskiyou Mountains of Curry County in south western Oregon near the town of Brookings ( $42.0575^{\circ}$  N,  $124.2864^{\circ}$  W) on

the coast (Figure 4.1) (Prospero et al., 2007). The Siskiyou mountains form part of the Klamath Mountain range (Franklin and Dyrness 1988). The vegetation in SOD infested areas is a mosaic of different vegetation types including mixed-evergreen, redwood (*Sequoia sempervirens*) and Douglas-fir (*Pseudotsuga menziesii*) forests with tanoak as the dominant SOD host.

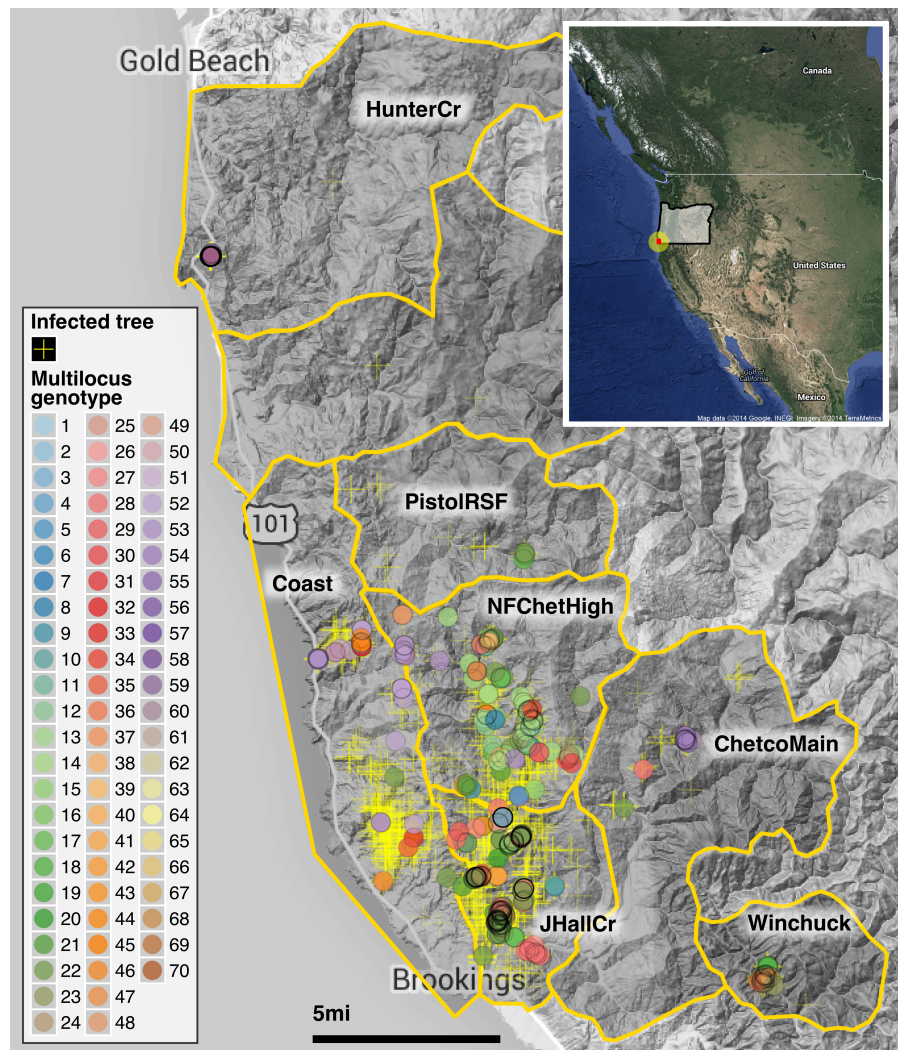


Figure 4.1: Spatial distribution of the SOD epidemic and multilocus genotypes of *Phytophthora ramorum* in Curry County, Oregon. The yellow crosses mark tanoak trees found positive for *P. ramorum* during aerial surveys. A total of 70 multilocus genotypes have been identified between 2001-2014 and are marked by color as shown in the legend. The abbreviations for regions shown in the map are explained in Table 4.1. The inset shows the placement of Curry county (red dot) in SW Oregon.

#### 4.3.2 Sampling

Commencing in 2001, 2-4 aerial surveys per year were conducted over the tanoak range by the Oregon Department of Forestry and the USDA Forest Service in Curry County. The survey detects recently killed tanoaks based on the reddish-brown color of foliage (Hansen et al., 2008). All trees identified by aerial surveys were ground checked and geographically referenced using a hand-held GPS instrument (Garmin GPS 12XL or 60CX, Garmin International, Olathe, KS). Bark or foliage samples were collected for determination of *P. ramorum* presence by culturing in the field and laboratory. Host plants within the area of the delimitation survey, generally 300 feet, were also inspected and sampled if they were symptomatic. Maps of distribution were prepared using ArcView GIS version 3.3 and ArcMap version 10.2 (Environmental Systems Research Institute, Redlands, CA).

#### 4.3.3 Isolation, identification and DNA extraction

Isolations were made from symptomatic plant tissue onto selective CARP agar (Difco corn meal agar, 10 ppm natamycin, 200pm NA-ampicillin, and 10 ppm rifampicin) (Prospero et al., 2007). Candidate *Phytophthora* cultures were transferred onto corn meal agar with 30 ppm  $\beta$ -sitosterol. *P. ramorum* identification was confirmed by microscopic inspection for presence of characteristic chlamydospores and deciduous sporangia (Werres et al., 2001). Genomic DNA was extracted using either the FastDNA SPIN kit (MP Biomedicals, LLC; 116540600) (Goss et al., 2009) or the cetyltrimethyl ammonium bromide (CTAB)-chloroform-isopropanol method (Winton and Hansen,

Abbreviation	Region name	Year	Number of isolates	MLGs detected (region specific)
JHallCr	Joe Hall Creek	2001, 2002, 2003, 2004, 2005, 2013, 2014	244	30 (19)
NFChetHigh Coast	North Fork Chetco Coastal Region	2003, 2012, 2013, 2014 2006, 2010, 2011, 2012, 2013, 2014	114 34	35 (19) 12 (7)
HunterCr	Hunter Creek; Cape Sebastian	2011	66	4 (4)
Winchuck	...	2012, 2013	35	9 (3)
ChetcoMain	...	2013, 2014	16	7 (1)
PistolRSF	Pistol River South Fork	2013	4	2 (0)
<b>Total</b>	-	<b>2001-2014</b>	<b>513</b>	<b>70 (53)</b>

Table 4.1: Summary of *P. ramorum* isolates sampled in Oregon forests and multilocus genotypes (MLG) observed across regions and years.

2001). Table 4.1 provides an overview of strains collected by year and region following regions as shown in figure 4.1.

#### 4.3.4 Genotyping, data validation, and harmonization

Five microsatellite loci were utilized in this analysis: PrMS6, Pr9C3, PrMS39, PrMS45, and PrMS43 (Grünwald et al., 2009, 2008b; Prospero et al., 2004, 2007). Genotyping (see specific protocols in supplementary text) of *P. ramorum* strains collected 2001-2012 occurred over several years and in several laboratories, with different protocols and sequencers. Consequently, a concerted effort was made to create a comprehensive dataset with identical allele calls. To detect errors, allele calls from all five genotyped loci were generated for a subsample of 40 isolates representing the most common multilocus genotypes from the culture collection, and then compared to data from participating laboratories. Three of the five loci, PrMS6, Pr9C3, and PrMS39 had identical allele calls between laboratories for the subsampled isolates. The remaining two loci, PrMS45 and PrMS43, had allele calls that differed by a single bp between laboratories. Data from PrMS45 and PrMS43 were therefore corrected to allow consistent comparisons of allele calls. Given the varied nature of the genotyping data described above genotyping of *P. ramorum* strains consists of two datasets including either 5 loci (2001-14) or a newly developed, multiplexed method including 14 loci (samples 2013-14) (Table 4.2). Details on both genotyping methods can be found in the supplementary text 4.7.1 and figure S4.6.

<b>SSR Locus</b>	<b>Dye</b>	<b>Product (bp)<sup>c</sup></b>	<b>Primer sequence<sup>b</sup></b>	<b>Final conc. (<math>\mu</math>M)</b>	<b>Rxn</b>
ILVOPrMS145abc <sup>f</sup>	6-FAM	167-257	Fwd6FAM-TGGCAGTGTCTCAACAGC Rev-GTTTATTCCCGTGAAACAGCGTATC	0.04	8-plex
PrMS39 <sup>d</sup>	NED	130-258	FwdNED-GCACGGCCAGAGATTGATAG Rev-GTTTATCTGCCGACGTGAAGAAGT	0.07	8-plex
PrMS9C3 <sup>d</sup>	PET	210-226	FwdVIC-TCACACCGAAGCAGCAACTCT Rev-GTTTAGCGGCACTACGGAAATACAT	0.04	8-plex
ILVOPrMS79 <sup>a,f</sup>	6-FAM	342-396	Fwd6FAM-AGGCCGAAAACGTCAGAAC Rev-GTTTCTCGAGGAGGTGGAAGTACG	0.15	8-plex
KI18 <sup>e</sup>	VIC	217-279	FwdPET-TGCCATCACAAACAAATCC Rev-GTTTGTGCTATCTTCCTGAAACGG	1.0	8-plex
KI64 <sup>e</sup>	NED	342-401	FwdNED-GCGCTAAGAAAGACACTCCG Rev-GTTTCAACATGTAGCCATTGCAGG	0.35	8-plex
PrMS45 <sup>d</sup>	VIC	138-186	FwdVIC-CGTGCTGCATCTGGTAGT Rev-GAAAAGTCCGGATTGGTTA	0.15	8-plex
PrMS6 <sup>d</sup>	PET	165-168	FwdPET-AATCGATCTCTGGTTTA Rev-TATAGCCCCAGCTGCAAACA	0.15	8-plex
ILVOPrMS131 <sup>f</sup>	VIC	146-414	FwdVIC-CGGCCGTTTTGTAAGTTTG Rev-GTTTCAGATCAAACCAAATCTGCTC	0.2	2-plex
KI82ab <sup>e</sup>	NED	95-243	FwdNED-CCACGTCAATTGGGTGACTTC Rev-GTTTCTGTACAAGTCACGACTCCC	0.2	2-plex
PrMS43 <sup>d</sup>	6-FAM	122-493	Fwd6FAM-AAATATGCAAAAAGGCAGGA Rev-GTTTCCGGTAGTACCTAGTCTGCTC	0.3	Simplex

Table 4.2: (Caption on Next Page)

Table 4.3: (Caption for Table 4.2) Newly multiplexed protocol for *P. ramorum* primer sequences of simple sequence repeat (SSR) loci and final concentrations used to determine multilocus genotypes for four clonal lineages. PrMS6, Pr9C3, PrMS39, PrMS45, and PrMS43 were utilized in this study as they were commonly genotyped across all laboratories. <sup>a</sup> ILVOPrMS79 amplifies three alleles in the NA1 lineage. The first two alleles are fixed and the third is polymorphic. <sup>b</sup> Reverse (Rev) primer includes PIG tail addition except for PrMS45 and PrMS6. Indicated in italic. <sup>c</sup> Product size range is for four lineages (EU1, EU2, NA1, NA2). Only the NA1 lineage has been reported in Curry County, OR forests. <sup>d</sup> Described by Prospero et al. (2004) and/or Prospero et al. (2007). <sup>e</sup> Described by Ivors et al. (2006). <sup>f</sup> Described by Vercauteren et al. (2010), and Vercauteren et al. (2011).

#### 4.3.5 Nursery populations

To determine if forest populations cluster with different nursery populations from Oregon or California, we used previously published data from our work to determine relationships among nursery and Curry County forest populations (Goss et al., 2009, 2011; Grünwald et al., 2009; Prospero et al., 2009, 2007).

#### 4.3.6 Data analysis

All individuals genotyped for this effort belonged to the NA1 clonal lineage (Grünwald et al., 2009). Thus, all analyses presented here focused on describing the clonal dynamic using model-free approaches that avoid violation of population genetic theory. Samples were grouped into different multilocus genotypes (MLGs) defined by the unique combination of alleles across all observed loci from the consensus five SSR loci genotyped across all years. For identification purposes, unique MLGs were then assigned an arbitrary number from 1 to the total number of observed MLGs. Population genetic analysis was conducted using the computer and statistical language R (R Core Team, 2014) using various packages as well as R functions written specifically for this project (see github link below). Graphs and figures were created using the R packages *ggplot2*, *ape*, *igraph*, *ggmap*, and *poppr* (Csardi and Nepusz, 2006; Kahle and Wickham, 2013; Kamvar et al., 2014b; Paradis et al., 2004; Wickham, 2009). Within-locus allelic diversity was analyzed across and within years and regions using the function *locus\_table()* from the R package *poppr* (Table S1) (Kamvar et al., 2014b). To address the temporal and spatial aspects of the data, populations were analyzed both

by year isolated and watershed region (Table 4.1; Fig. 4.1). Watershed regions were drawn with ArcMap version 10.2 (Environmental Systems Research Institute, Redlands, CA). The regions represent drainages or portions of drainages in which infected trees were discovered as the disease progressed over time. In most cases, ridgelines dividing drainages formed the boundary of a region. These regions were saved as shapefiles and imported into R with *rgdal* (Bivand et al., 2014).

Genotypic diversity was analyzed within and across years and populations, with the Shannon-Wiener index ( $H$ ) and the Stoddard and Taylor's index ( $G$ ), (Shannon, 2001; Stoddart and Taylor, 1988). Both  $G$  and  $H$  measure genotypic diversity, combining richness and evenness. If all genotypes are equally abundant, then the value of  $G$  will be the number of MLGs and the value of  $H$  will be the natural log of the number of MLGs. Both  $G$  and  $H$  are used as they weigh more or less abundant MLGs more heavily, respectively (Grünwald et al., 2003). Evenness was calculated as  $E_5$ , which is an estimator of evenness that utilizes both  $H$  and  $G$  that gives a ratio of the number of abundant genotypes to rare genotypes (Grünwald et al., 2003; Ludwig and Reynolds, 1988; Pielou, 1975). These were calculated with the R packages *poppr* and *vegan* (Kamvar et al., 2014b; Oksanen et al., 2013). Confidence intervals were calculated using the R package *boot* with 9,999 bootstrap resamplings (Canty and Ripley, 2015). Richness, or the expected number of MLGs ( $eMLG$ ), was calculated using rarefaction from the R packages *poppr* and *vegan* (Heck et al., 1975; Hurlbert, 1971). Some statistics (AMOVA, genotypic diversity, index of association, allelic diversity, and Nei's distance) were also performed on clone-censored data where each MLG was represented once per population hierarchy.

Because the analysis of genotypic diversity, richness and evenness is agnostic to specific alleles within MLGs, assessment of genetic relatedness between MLGs was performed using the function `bruvo.dist()` using *poppr*, which calculates Bruvo's genetic distance, utilizing a stepwise mutation model for microsatellite loci (Bruvo et al., 2004; Kamvar et al., 2014b). This distance thus gives a more fine-scale picture of relationships between individuals than band-sharing models. These relationships were visualized with minimum spanning networks generated using the R packages *igraph* and *poppr* (Csardi and Nepusz, 2006; Kamvar et al., 2014b).

If the epidemic had a single origin, a correlation between genetic and geographic distance would be expected as populations acquire mutations over time and clonally diverge regardless of rates of spread. Divergence is affected by rates and distance of spread where long-distance dispersal or low rates of mutation would lead to less divergence and thus lower correlations between genetic and geographic distances. This was tested by performing Mantel tests across all hierarchical levels in the data set utilizing the function `mantel.randtest()` in the R package *ade4* between Bruvo's distance as described above and Euclidean distances between geographic coordinates (Dray and Dufour, 2007; Mantel, 1967). *P*-values were calculated using 99,999 bootstrap replicates.

As the eradication efforts destroy the immediate habitat in an infected area, one question that we wanted to address was whether or not genotypes were clustering to specific regions or if they were evenly spread throughout Curry County (Prospero et al., 2007). This was tested using three methods: bootstrap analysis of Nei's genetic distance, Analysis of MOlecular VAriance (AMOVA), and Discriminant Analysis of Prin-

incipal Components (DAPC) in the R packages *poppr*, *ade4*, and *adegenet* (Excoffier et al., 1992; Jombart et al., 2010; Kamvar et al., 2014b). The bootstrap analysis utilized 10,000 bootstrap replicates treating loci as independent units with the function `aboot()` in *poppr* and was visualized as an unrooted neighbor-joining tree in *figtree* v. 1.4.2 (Figure 4.5). AMOVA utilizes a distance matrix between genotypes for which hierarchical partitions are defined and attempts to analyze the variation within samples, between samples, between subpopulations within populations and finally between populations. In this case, we used both the hierarchies of samples within years within regions and samples within regions within years. DAPC is a multivariate, model-free approach to clustering based on prior population information (Jombart et al., 2010). This allows us to analyze the population structure by assessing how well samples can be reassigned into previously defined populations. Both DAPC and AMOVA were run with and without Hunter Creek and Pistol River South Fork due to isolated genotypes and small sample size, respectively. For the DAPC analysis, these removed populations had their origins predicted from the DAPC object using the function `predict.dapc` in the R package *adegenet* (Jombart et al., 2010).

Since DAPC is sensitive to the number of principal components used in analysis, the function `xvalDapc()` from the R package *adegenet* was used to select the correct number of principal components with 1,000 replicates using a training set of 90% of the data. The number of principal components was chosen based on the criteria that it had to produce the highest average percent of successful reassignment and lowest root mean squared error (Jombart et al., 2010). Significant deviations from random population structure was tested in AMOVA utilizing the function `randtest()` from

the R package *ade4* with 9,999 bootstrap replicates (Dray and Dufour, 2007).

All data and R scripts to reproduce the analyses shown here are deposited publicly on github ([https://github.com/grunwaldlab/Sudden\\_Oak\\_Death\\_in\\_Oregon\\_Forests](https://github.com/grunwaldlab/Sudden_Oak_Death_in_Oregon_Forests)) and citable (DOI: 10.5281/zenodo.13007).

## 4.4 Results

### 4.4.1 Demographic pattern and genetic diversity

The epidemic has expanded over time from the initial focus in Joe Hall Creek NE of Brookings, Oregon mostly north (first to N Fork Chetco High) and northwest (Coast, Pistol River South Fork), but also east (Chetco Main and Winchuck) (Fig. 4.1; Table 4.1). To date a total of 70 multilocus genotypes have been found in forest populations (Table 4.1). MLG 22 is most abundant and the only MLG detected across the whole period (although it was not sampled in every year) (Fig. 4.2). MLG 59, the second most abundant MLG, was only detected in 2011 and has a high frequency due to the sampling design applied: all 2011 strains were sampled in one concentrated area in the northwestern sampling range geographically distant from any other location (Fig. 4.2). Given that sampling strategies for some years were not comprehensive, samples from some years have to be interpreted with caution (e.g., 2005-6, 2010-11). Samples from 2013 and 2014 are sampled from all regions and can be considered more representative.

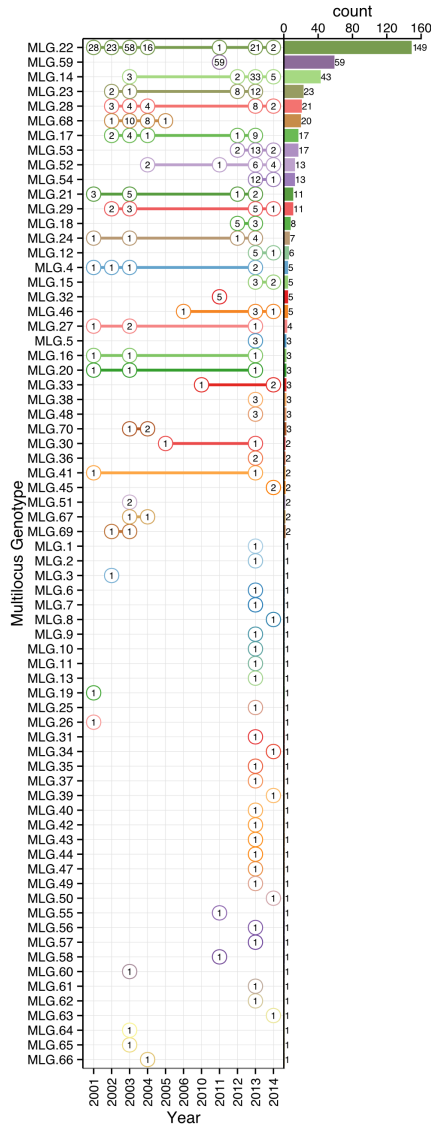


Figure 4.2: Rank distribution of multilocus genotypes (MLGs) of *P. ramorum* and recovery per year. The vertical axis denotes unique MLGs detected in the whole data set with decreasing abundance as indicated by the barplot on the right side. The horizontal axis indicates year of sampling. Each numbered circle represents the number of observations of each MLG with lines connecting genotypes found in multiple years.

Allelic and genotype diversity within loci revealed that PrMS43 had, on average, the highest number of alleles ( $n = 18$ ). All other loci had 5 or fewer alleles with a moderate to high amount of diversity (Table S2). Nevertheless, the genotype accumulation curve showed a slight plateau, indicating that we have enough power in our data to describe a significant number of MLGs (Fig. S4.7). Genotypic diversity ( $H = 2.98$ ,  $G = 8.64$ ), evenness ( $E_5 = 0.41$ ), and richness ( $eMLG = 7$ ) were low as expected for a clonal population slowly accumulating mutations over space and time (Table S3). A pattern of increasing diversity across years (with number of MLGs not fewer than 10) was also observed (Table S3). The minimum spanning network showed that MLGs 17, 22, and 28 clustered in the center of the network and had the highest number of connections to other genotypes in the forest populations (Fig. 4.3). Most genotypes were connected to their immediate neighbors by a genetic distance of 0.05 or the equivalent of one mutational step across 5 diploid loci.

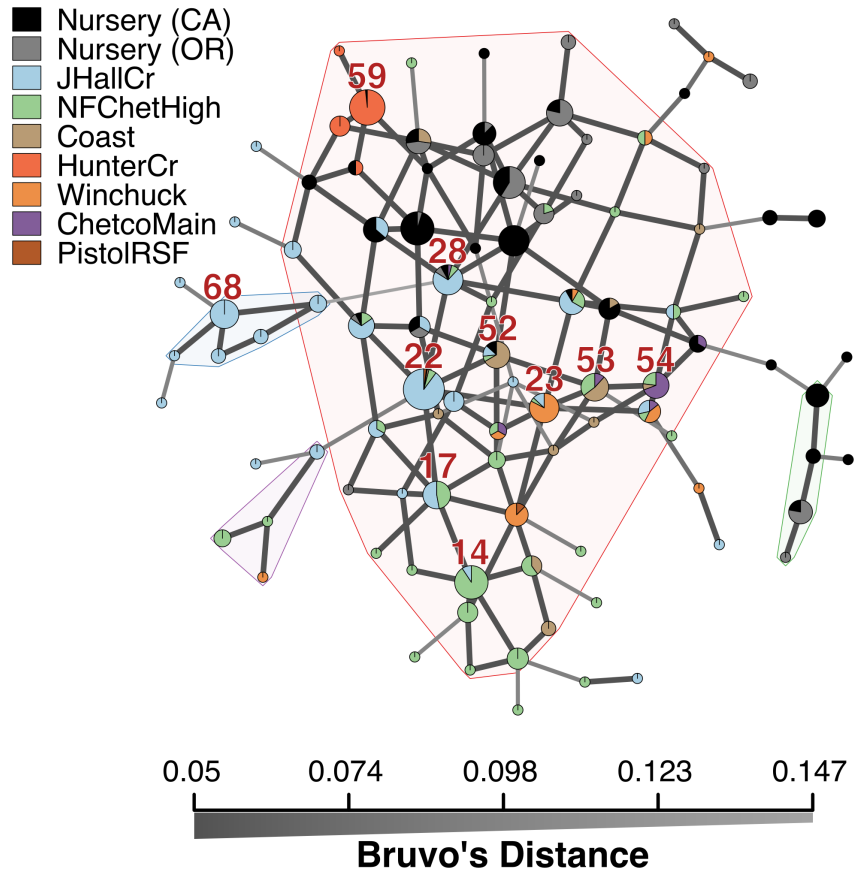


Figure 4.3: Minimum spanning network based on Bruvo's genetic distance for microsatellite markers for *P. ramorum* populations. Nodes (circles) represent individual multilocus genotypes. The 10 most abundant forest genotypes are labeled with their MLG designation. Node colors represent population membership proportional to the pie size. Node sizes are relatively scaled to  $\log_{1.75} n$ , where  $n$  is the number of samples in the nodes to avoid node overlap. Edges (lines) represent minimum genetic distance between individuals determined by Prim's algorithm. Nodes that are more closely related will have darker and thicker edges whereas nodes more distantly related will have lighter and thinner edges or no edge at all. Reticulation was introduced by finding exact ties in genetic distance after Prim's algorithm was run. Subgroups of  $>3$  MLGs where all nodes are no more than one mutational step ( $d = 0.05$ ) away from its neighbors, are highlighted in arbitrary colors.

#### 4.4.2 Spatial Correlation

A Mantel test revealed significant correlations of genetic distance and geographic distance for most samples collected after 2003 (Table 4.4). When partitioned by year, this correlation appears to increase and become more pronounced with the progression of the epidemic. When partitioned by region, those that are closer to the origin of the epidemic (Joe Hall Creek and N Fork Chetco River) show significant correlation. When the overall mantel test was run without Hunter Creek, the correlation coefficient was reduced (0.175), but was still significant ( $p = 0.0001$ ).

#### 4.4.3 Population differentiation

Cluster analysis of populations with respect to year using Nei's genetic distance showed no significant (>70%) bootstrap support for any clades, but does show that these tend to cluster by region as opposed to year (Fig. S4.8). AMOVA analysis revealed significant population structure between regions on both clone-corrected (with respect to hierarchy) and uncorrected data sets (Table 4.5). Significant structure was only found between years within regions on the uncorrected data set. Both patterns were observed without Hunter Creek and Pistol River South Fork isolates. DAPC clustering showed that the first discriminant component separated Hunter Creek from all other regions and the second discriminant component shows a gradient from Joe Hall Creek to the coast (Fig. 4.4). This distinction was reflected in the percent of correct posterior assignment of isolates to their original populations. Over the whole data set there was an 81.5% assignment-success rate. Hunter Creek received 100% successful reassign-

	<b>2001</b>	<b>2002</b>	<b>2003</b>	<b>2004</b>	<b>2005</b>	<b>2006</b>	<b>2010</b>	<b>2011</b>	<b>2012</b>	<b>2013</b>	<b>2014</b>	<b>Pooled</b>
JHallCr	0.06	0.24	0.14*	0.28*	NaN	-	-	-	-	0.18~	NaN	0.14*
NFChetHigh	-	-	NaN	-	-	-	-	-	0.68	0.41*	-0.23	0.35*
Coast	-	-	-	-	NaN	NaN	NaN	NaN	0.06	-	-	0.06
HunterCr	-	-	-	-	-	-	-	-	-	-	-	-
Winchuck	-	-	-	-	-	-	-	-	0.41~	0.03	-	0.11
ChetcoMain	-	-	-	-	-	-	-	-	-	0.53	NaN	0.63*
PistolRSF	-	-	-	-	-	-	-	-	-	0.94	-	0.94
Pooled	0.06	0.24	0.13*	0.28*	NaN	NaN	0.87*	0.59*	0.15*	0.14~	<b>0.52*</b>	-

Table 4.4: Table of correlation coefficients generated across forest regions and years of *P. ramorum* isolates using the Mantel test. Euclidean distances were calculated from geographic coordinates while genetic distance was based on Bruvo's distance. Significance of values are based on 99,999 Monte-Carlo permutations and marked as follows: ^  $\leq 0.05$ , ~  $\leq 0.01$ , \*  $\leq 0.001$ , - = no data, NaN = insufficient data for analysis.

ment. Joe Hall Creek, Winchuck, and Coast all had >85% successful reassignment whereas Chetco Main, North Fork of the Chetco, and Pistol River South Fork all had <69% successful reassignment (Fig. S4.9). The isolation of the Hunter Creek isolates in the DAPC analysis was found to be mainly driven by allele 493 at locus PrMS43 (Fig. S4.10). The only other population to share this allele was Joe Hall Creek where it was present in a total of 4 isolates, and only isolates found in the coastal region or North Fork Chetco contained the allele 489, which is one mutational step away in a stepwise mutation model of a tetranucleotide repeat locus. When DAPC was run without Hunter Creek and Pistol River South Fork data, percent successful reassignment for all regions did not change significantly. Prediction of sources for the Hunter Creek data revealed that over 98% of the genotypes were assigned to the Coast with a 99% probability.

Heirarchy	df	Sum of squares	Variation (%)	P	$\phi$ statistic
<b>Region by year</b>					
Between region	10 (10)	160 (21)	11.6 (3)	0.366 (0.175)	0.448 (0.101)
Between year within region	12 (12)	59.5 (19.1)	33.3 (7.07)	1e-04 (2e-04)	0.376 (0.0729)
Within year within region	490 (129)	281 (141)	55.2 (89.9)	1e-04 (1e-04)	0.116 (0.03)
<b>Year by region</b>					
Between year	6 (6)	197 (23)	45 (12.3)	1e-04 (1e-04)	0.496 (0.12)
Between region within year	16 (16)	22.5 (17.2)	4.56 (-0.283)	1e-04 (0.446)	0.0829 (-0.00323)
Within region within year	490 (129)	281 (141)	50.4 (88)	1e-04 (1e-04)	0.45 (0.123)

Table 4.5: AMOVA table generated comparing *P. ramorum* isolates for two different hierarchies, year within region and region within year, respectively. Results are rounded to three significant figures. Clone corrected results are provided in parentheses. P values are based on 9,999 permutations.

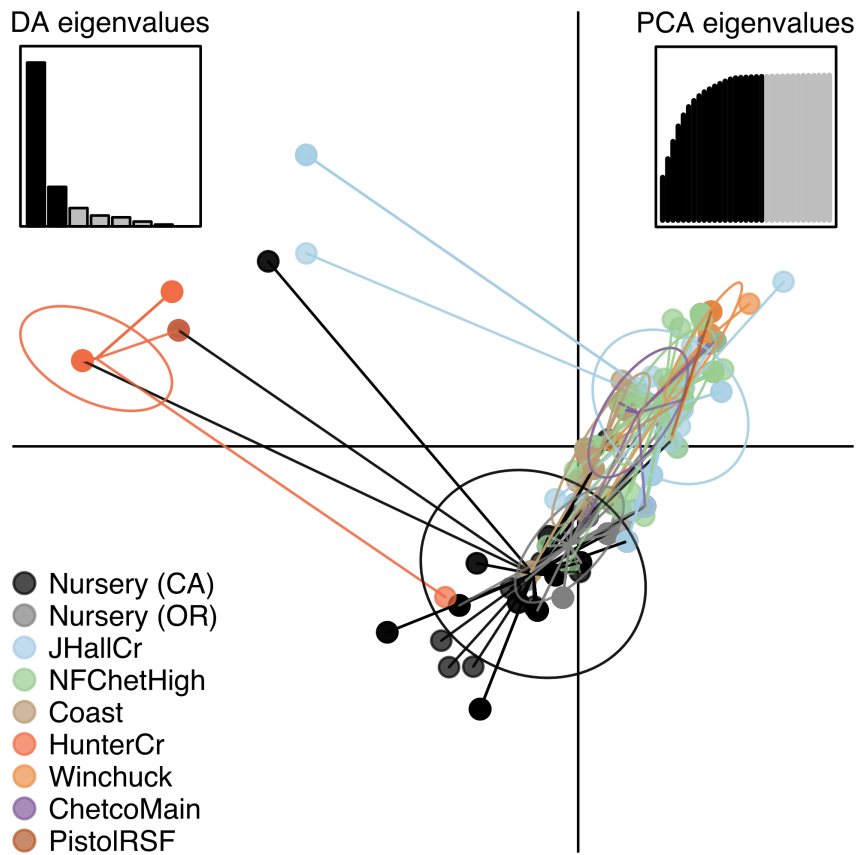


Figure 4.4: Scatterplot from DAPC of the first two principal components discriminating *P. ramorum* populations by regions. Points represent individual observations. Colors and lines represent population membership. Inertia ellipses represent an analog of a 67% confidence interval based on a bivariate normal distribution.

#### 4.4.4 Clustering of forest with nursery populations

We used previously published data to determine if nursery populations in California or Oregon could have been source populations for the Oregon forest epidemic (Goss et al., 2009, 2011; Grünwald et al., 2009; Prospero et al., 2009, 2007). Nursery data included 40 MLGs across 216 samples of NA1 clones. Of these 40, 12 MLGs matched the forest sample and 28 MLGs were unique to the nurseries. The only region that did not contain genotypes that matched those found in nurseries was Pistol River South Fork. When considering those 12 genotypes that were present in both data sets, with the exception of Joe Hall Creek, all genotypes were first isolated from nurseries before discovery in the forest. At the most variable locus, PrMS43, both nursery populations had the allele 281 at frequencies of 4.5% and 4.9% for CA and OR, respectively. This allele was not observed in the forest population. Both populations contained allele 489 at >10% frequency and the CA nursery population contained allele 493 at a frequency of 1.4%.

When nursery genotypes were added to the minimum spanning network, MLGs found at Hunter Creek, previously isolated in the network, connected by only a single MLG from the coast, gained more connections to nursery MLGs. Clustering with Nei's distance revealed the Nursery isolates from CA consistently clustering closest with Hunter Creek isolates in both clone-corrected and uncorrected data sets (Fig. 4.5). DAPC clustering revealed a decrease in overall assignment-success rate at 78%. The nursery isolates received 74% and 83% assignment success for CA and OR nurseries, respectively.

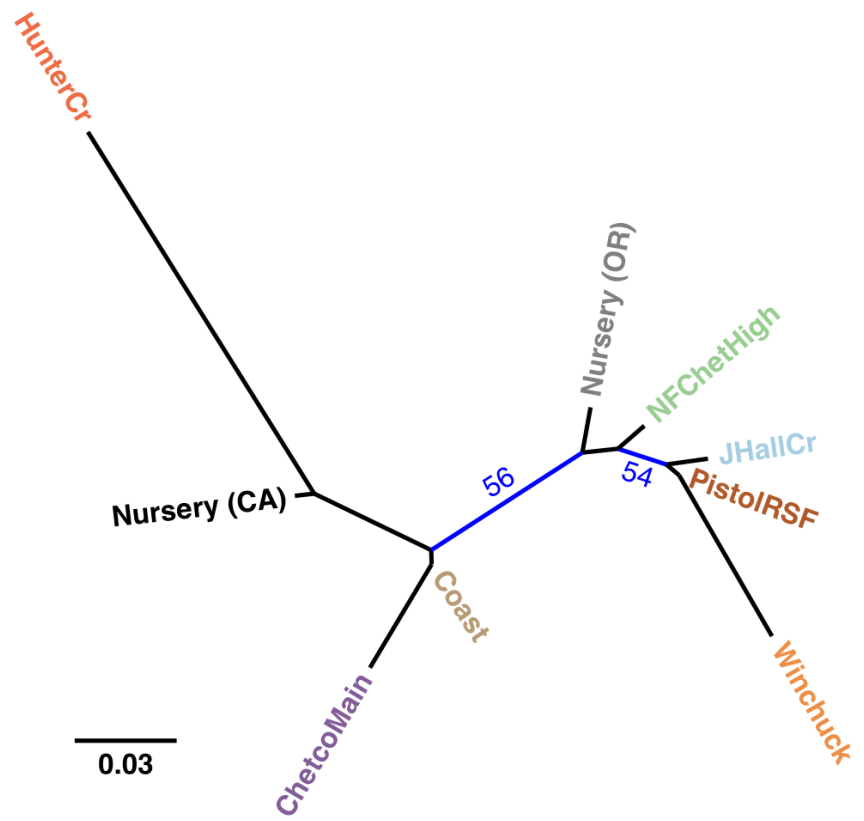


Figure 4.5: Unrooted, neighbor-joining tree with 10,000 bootstrap replicates of Nei's genetic distance for *P. ramorum* populations defined by region. Tip labels are colored by region. Branches with bootstrap values greater than 50% are shown in blue. Nursery populations are shown as originating from California (CA) or Oregon (OR).

The assignment successes for the regions before or after inclusion of nursery data changed less than 5% for all regions except for the coast, which saw a decrease of 17.6% when nursery populations were included (Fig. S4.9). Prediction of sources for nursery genotypes against the forest data revealed that 48% of these nursery isolates were predicted to share membership with the coast at  $\geq 95\%$  probability (Fig. S4.11, S4.12). A total of 3.2% of the isolates were predicted to share membership with Hunter Creek at  $\geq 99.9\%$  membership probability. Furthermore, 21.75% of the nursery data could not be assigned to any of the forest populations at  $>60\%$  probability.

Since 3.2% of the nursery isolates had a very strong signal for Hunter Creek, we predicted sources for Hunter Creek isolates when considering nursery isolates. This approach determines if Hunter Creek isolates cluster more readily with nursery or coast populations. Indeed, 92% of the Hunter Creek isolates were predicted to share membership with California nurseries at  $\geq 99\%$  membership probability (Fig. S4.13). No Hunter Creek isolate was predicted to share membership with a forest population at  $>0.45\%$  membership probability.

#### 4.5 Discussion

To date populations monitored from 2001-14 show presence of only the NA1 clonal lineage observed previously (Prospero et al., 2009, 2007). The fact that individuals belonging to the EU1 and NA2 clonal lineages have not been found in Oregon forests, despite their presence on the west coast from British Columbia to California is welcome news (Goss et al., 2009, 2011; Grünwald et al., 2012). The lack of EU1 or NA2 isolates

provides evidence that monitoring for *P. ramorum* in nurseries by federal and state agencies is helping avoid emergence of new clones in Oregon's Forests.

Our analysis provides support for a most parsimonious scenario of two introductions into Curry county from nurseries: one initial introduction into Curry County sometime before detection of the first infected tanoaks in 2001 from California (or less likely Oregon) nurseries followed by a second introduction into the Hunter Creek area again from nurseries. The relative position of the nursery populations in the minimum spanning network and DAPC scatter plot (Fig. 4.3, 4.4) suggest that the introductions from nurseries were rare, though more even sampling and migration models could disprove this hypothesis. Since 2001, the epidemic has spread clonally throughout Southwestern Curry County mostly north, but also west, towards the coast, and southeast. This clonal spread of the pathogen from the Joe Hall area is supported partially by Mantel tests showing significant levels of isolation by distance in years following 2002 (Table 4.4) along with significant AMOVA results across regions (Table 4.5). The populations sampled in 2011 in Hunter Creek (Cape Sebastian) appear to have originated from a new source and cluster into a distinct group based on DAPC (Fig. 4.4). Based on the minimum spanning network, this population would appear isolated in the epidemic if it were not for MLG 32, which is connected with MLG 33 (found on the coast in 2010) by one mutational step at locus PrMS43. This, in turn, is connected with the other MLGs from Hunter Creek by one mutational step at locus PrMS39. When considering clustering via Bruvo's distance in combination with data from nursery populations, however, these genotypes from Hunter Creek appear to be more similar to California nursery populations (Fig. 4.3) than Oregon forest populations. Predictions

based on DAPC place samples from Hunter Creek as coming from California nurseries (Fig. S4.13). This, in combination with the observation that purely forest genotypes (i.e. those only found in the forest) are connected to Hunter Creek genotypes through nursery genotypes, indicates a possible contribution from nursery populations to the epidemic. This is supported by the observation that all population level clustering, with and without clone correction, places the Hunter Creek isolates adjacent to the nursery isolates from CA (Fig. 4.4, 4.5). This appears to be driven by the high frequency of allele 246 at locus PrMS39, which interestingly appears to segregate in an east to west fashion and is increasing in frequency over time (Fig. S4.14, S4.15). This, along with the results from the DAPC clustering and subsequent prediction (Fig. S4.11, S4.12) provide weak support for a potential third introduction into the coastal region from nurseries sometime after the Hunter Creek introduction event.

An interesting aspect is the observation that there appeared to be more than one cluster of genotypes introduced into the Joe Hall area during the early stages of the epidemic. The two dominant clusters that appeared were the ones that contained MLG 22 and MLG 68. The former has been found in the most recent sampling year, whereas the latter has not been observed since 2005 or beyond the Joe Hall area. This latter group was also the most distantly related group overall, more distant than some nursery genotypes. While it is clear that the eradication effort has not been entirely successful, there is some evidence that it is having an effect as a major genotype cluster has effectively been eradicated, although disappearance of MLGs could also be explained by being less fit than lineages dominating now.

The Curry County epidemic is in many ways different from the epidemic in Cali-

fornia. When introduced into California in the mid 1990's, the causal agent of sudden oak death was unknown and thus gave it time to clonally expand and diversify as management strategies in natural forest systems were limited (Rizzo et al., 2002). With the foresight of the epidemic in central California, the ODF was able to implement a quarantine effort against the import of hosts as soon as the causal agent was known (A Kanaskie, pers. comm.). This quarantine along with aggressive eradication efforts have affected the spread of *P. ramorum* (Mascheretti et al., 2008). Drawing conclusions from previous population studies in California and applying them to the Oregon epidemic should be undertaken with great care given the drastically differing management scenarios (Mascheretti et al., 2009, 2008).

Our work has some inherent drawbacks. Given the cost of aerial surveys and subsequent ground crew work, and the fact that trees are eradicated once found, populations are not hierarchically sampled across all years. The destructive nature of the management approach means that it was not possible to conduct controlled ecological experiments focusing on effects of climate and rainfall on the spread of disease as was possible in California trials (Eyre et al., 2013). In addition, most of our work only used 5 microsatellite loci for genotyping. Ideally, more loci should have been used as was done in other studies (Croucher et al., 2013). Although only 5 loci were used, clear patterns of population dynamics in space and time emerged and the MLG accumulation curve supported the fact that loci are informative. Finally, the populations genotyped here are clonal and belong to the NA1 clonal lineage. Thus, much of the analytical power provided by population genetic theory does not apply given that basic assumptions would be violated (Grünwald and Goss, 2011). Our work

uses appropriate methods to infer patterns that are model free, yet informative such as spatial clustering. Thus, we believe that this work provides novel and important insights into the *P. ramorum* population biology in the Siskiyou forest. Our data indicates that there might have been at least two introductions into Oregon forests from nurseries. The nature of the data does not allow inference of directional migrations given the uneven sampling strategy and moderate number of loci used across all years. We are currently exploring genotyping-by-sequencing (GBS) as a method that could provide further detail on how these populations evolved over space and time (Elshire et al., 2011). GBS can provide richer detail by providing codominant SNP data across several thousand loci sampling the whole genome.

#### 4.6 Acknowledgements

This work was supported in part by US Department of Agriculture (USDA) Agricultural Research Service Grant 5358-22000-039-00D, USDA APHIS, the USDA-ARS Floriculture Nursery Initiative, the Oregon Department of Agriculture/Oregon Association of Nurseries (ODA-OAN) and the USDA-Forest Service Forest Health Monitoring Program.

## 4.7 Supplementary Material

### 4.7.1 Supplementary Text

For the years up to and including 2012, the multilocus genotype (MLG) of each *P. ramorum* strain was determined based on microsatellite analysis of five loci, PrMS6, Pr9C3, PrMS39, PrMS45 and PrMS43, using previously published protocols (Grünwald et al., 2009, 2008b; Prospero et al., 2004, 2007). Multilocus genotyping of *P. ramorum* strains collected in 2013 and 2014 included an extra nine loci, KI18, KI64, KI82a, KI82b, ILVOPrMS79, ILVOPrMS131, ILVOPrMS145a, ILVOPrMS145b, ILVOPrMS145c which are amplified by an additional six primer pairs (Ivors et al., 2006; Vercauteren et al., 2010, 2011). The locus ILVOPrMS79, amplifies up to three alleles, however two separate loci have yet to be described (Vercauteren et al., 2011). The addition of nine loci to the genotyping assay coincided with the discovery by the Oregon Department of Agriculture of an EU1 *P. ramorum* isolate in a Curry County nursery in 2012. Preceding 2012, only NA1 isolates had been found in Curry County. Because different loci are polymorphic for different clonal lineages, the entire panel of 14 loci was necessary to adequately describe the *P. ramorum* population in the event that multiple lineages were discovered in the forest.

Methods for genotyping the 2013 and 2014 *P. ramorum* strains with all 14 loci use new multiplex protocol. Previously published primers were modified by the addition of a 5' PIG tail "GTTT" to reverse primers in an effort to reduced stutter peaks and hence to better facilitate allele scoring (Table 4.2) (Brownstein et al., 1996). In two cases (PrMS45, PrMS6), a PIG tail was not added to reverse primers to simplify

scoring of overlapping alleles. Also, where a T residue was already present at the 5' end of a reverse primer, as in the case of KI18, a "GTT" was added instead of "GT<sub>3</sub>". Forward primers were assigned fluorescent labels, 6-FAM, NED, VIC, or PET, to facilitate separation of overlapping markers (Table 4.2). Primer concentrations were determined by visual inspection of electropherograms (Table 4.2).

Amplification of all 14 loci was separated into three reactions (8-plex, 2-plex and simplex). The simplex reaction amplified the PrMS43 locus using methods described earlier (Grünwald et al., 2009; Prospero et al., 2007). The 8-plex and 2-plex amplified the remaining loci and were performed under identical conditions with the exception of primers and primer concentrations (Table 4.2). For the multiplex reactions, the QIAGEN Type-it Mutation Detect PCR Kit (QIAGEN, 206343, Valencia, CA) was used. Multiplex PCR reactions were performed in 5 μl volumes with 10ng template DNA and 1X final buffer concentration. Amplifications were run on a Veriti thermal cycler (Life Technologies, Grand Island, NY) with an initial denaturation at 95 °C for 5 min, followed by 33 cycles of 95 °C for 30 s, 60 °C for 90 s, and 72 °C for 20 s, and a final extension at 60 °C for 30 min. Genotyping prior to 2012 included three reference DNA lineages (EU1, NA1, and NA2). After 2012, a fourth lineage (EU2) was added as a reference (Poucke et al., 2012).

Electrophoresis and visualization of all microsatellites were performed on ABI3100, ABI3100 Avant, or ABI3130 genetic analyzers (Applied Biosystems). For evaluation of the loci, genotyped prior to 2013, the PCR products were diluted 10 times in ultrapure H<sub>2</sub>O and 1.5 μl of diluted product was added to both 8.5 μl of Hi-Di™ Formamide (Applied Biosystems, 4311320) and 0.25 μl of GeneScan™ 500 LIZ™ size standard

(Applied Biosystems, 4322682). The simplex reaction (PrMS43) was also diluted 10 times while the 8-plex and 2-plex products were diluted 75 times. After dilution, 2.5  $\mu$ l of the 8-plex, 2-plex and simplex products were added to 7.5  $\mu$ l of Hi-Di<sup>TM</sup> Formamide containing GeneScan<sup>TM</sup> 500 LIZ<sup>TM</sup> size standard at a ratio of 6  $\mu$ l size standard to 1 ml Hi-Di<sup>TM</sup> Formamide. Allele sizing was determined using GeneMapper<sup>®</sup> v3.7 and v5.0 software (Applied Biosystems).

#### 4.7.2 Supplementary Figures

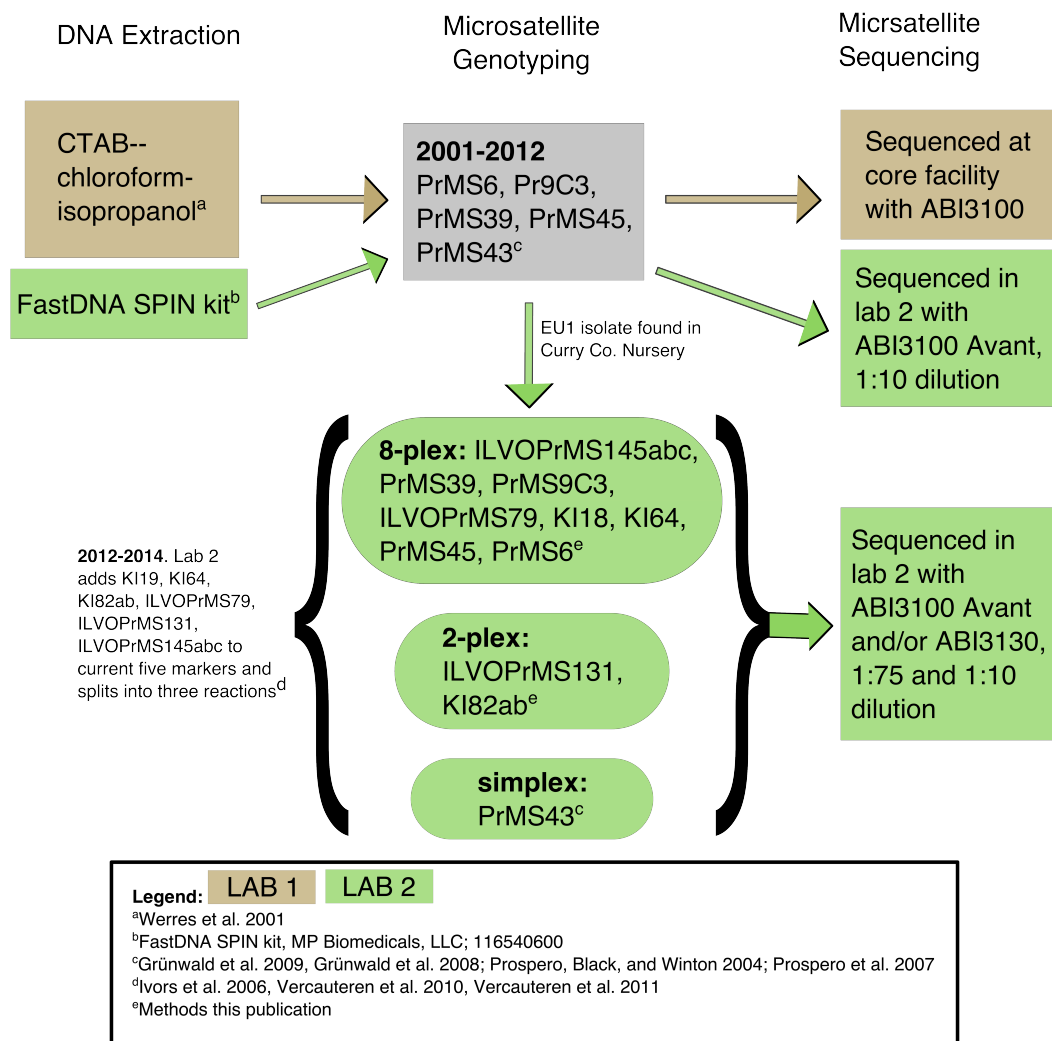


Figure 4.6: Diagram of DNA extraction, genotyping, and sequencing protocols utilized by two labs from 2001 to 2014. See supplementary text for details.

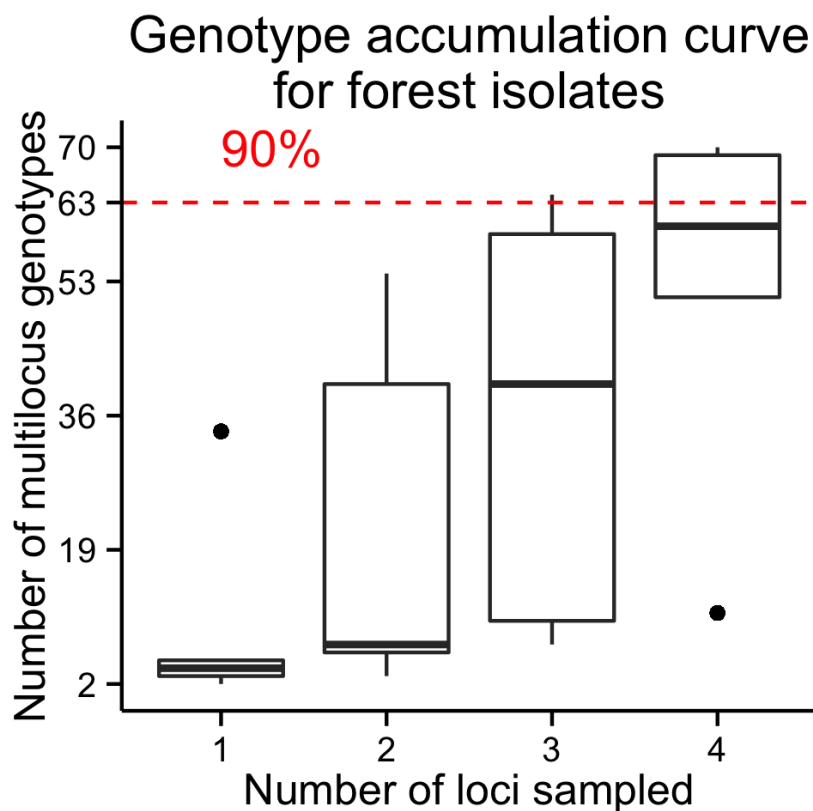


Figure 4.7: Genotype accumulation curve for OR forest *P. ramorum* isolates. The vertical axis denotes the number of observed MLGs, from 0 to the observed number of MLG in the forest populations, for a number of loci, indicated on the horizontal axis, randomly sampled without replacement. Each boxplot contains 1,000 random samples representing different possible combinations of  $n$  loci. The horizontal red dashed line represents 90% of MLG resolution.

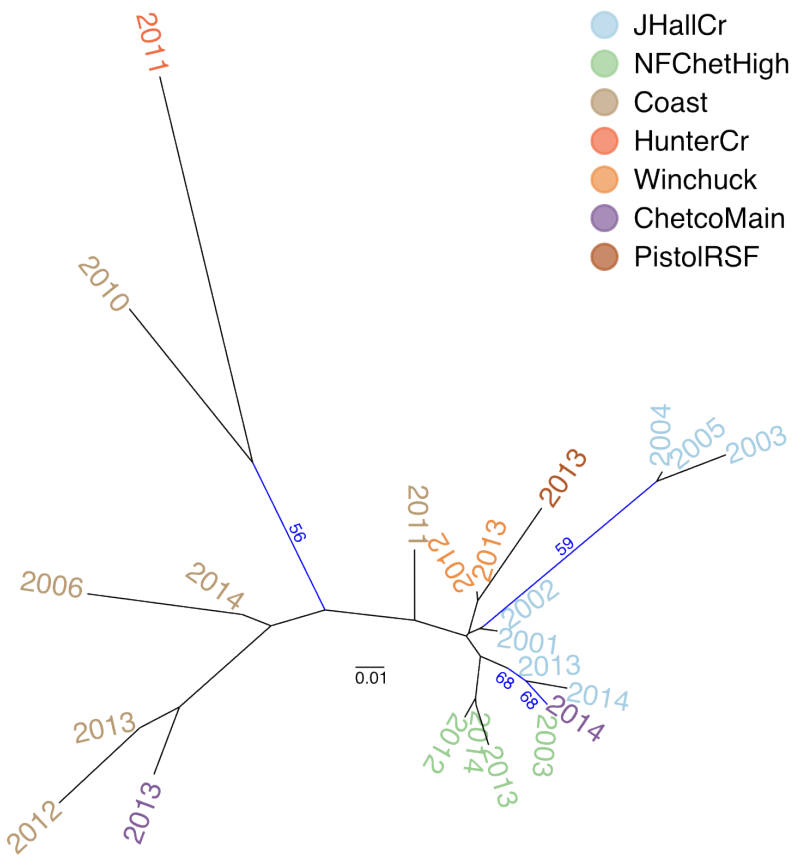


Figure 4.8: Neighbor joining tree based on Nei's distance of the forest *P. ramorum* isolates by region with respect to year. Bootstrap values  $> 50\%$  of 10,000 replicates are shown in blue.

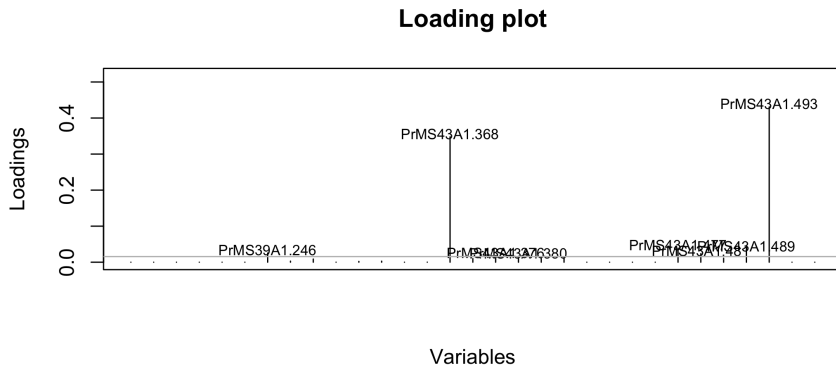


Figure 4.9: Fractions of posterior population assignments from DAPC clustering of *P. ramorum* isolates from forest populations. The horizontal axis represents the fraction of samples whose posterior group membership matched their prior group membership on the vertical axis. Shape indicates presence or absence of nursery populations in the DAPC.

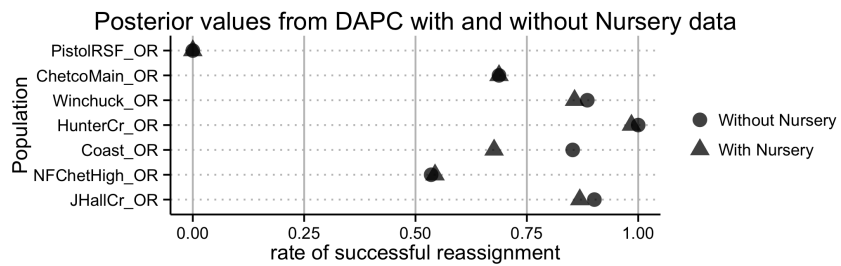


Figure 4.10: Loading plot from DAPC of *P. ramorum* from forest populations showing the contribution of alleles to the first DAPC eigenvalue separating Hunter Creek isolates from all other regions.

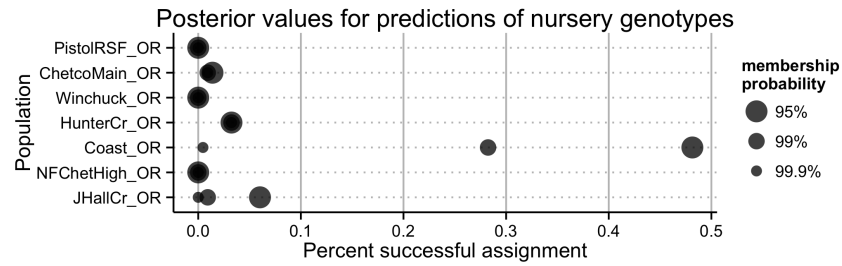


Figure 4.11: Prediction of nursery genotypes of *P. ramorum* into forest watershed regions. The horizontal axis indicates the fraction of nursery genotypes to be predicted to be similar to the populations on the vertical axis with a 95, 99, and 99.9% probability as indicated by the size of the points.

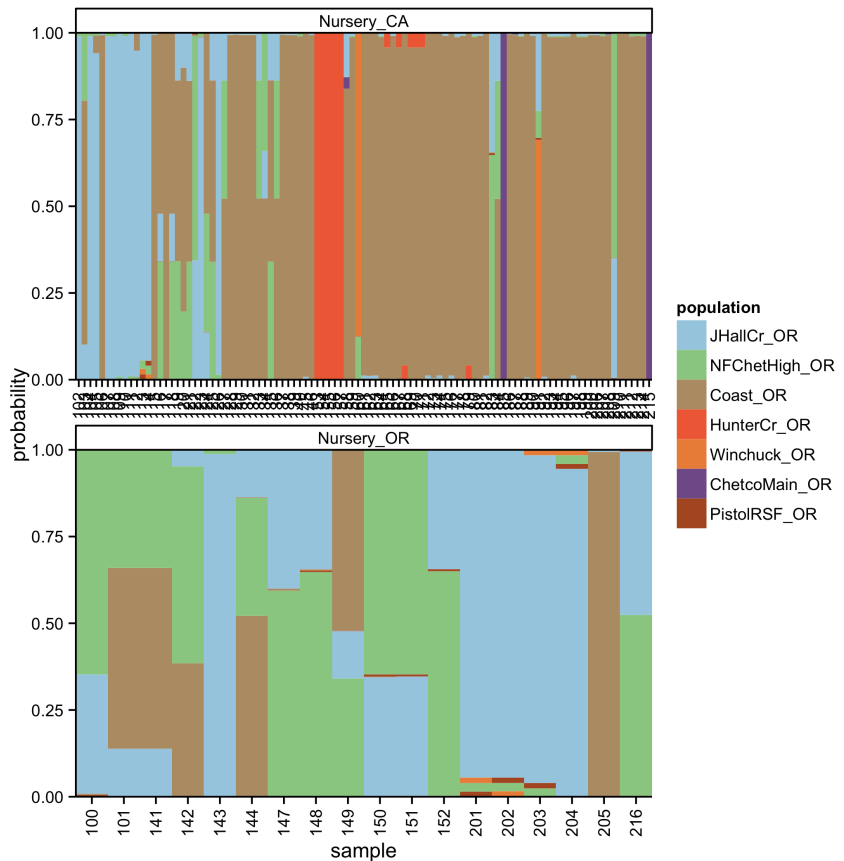


Figure 4.12: Graphical representation of prediction of nursery isolates of *P. ramorum* into forest watershed regions. Each column represents a different isolate. Colors within the columns represent membership probabilities from forest populations.

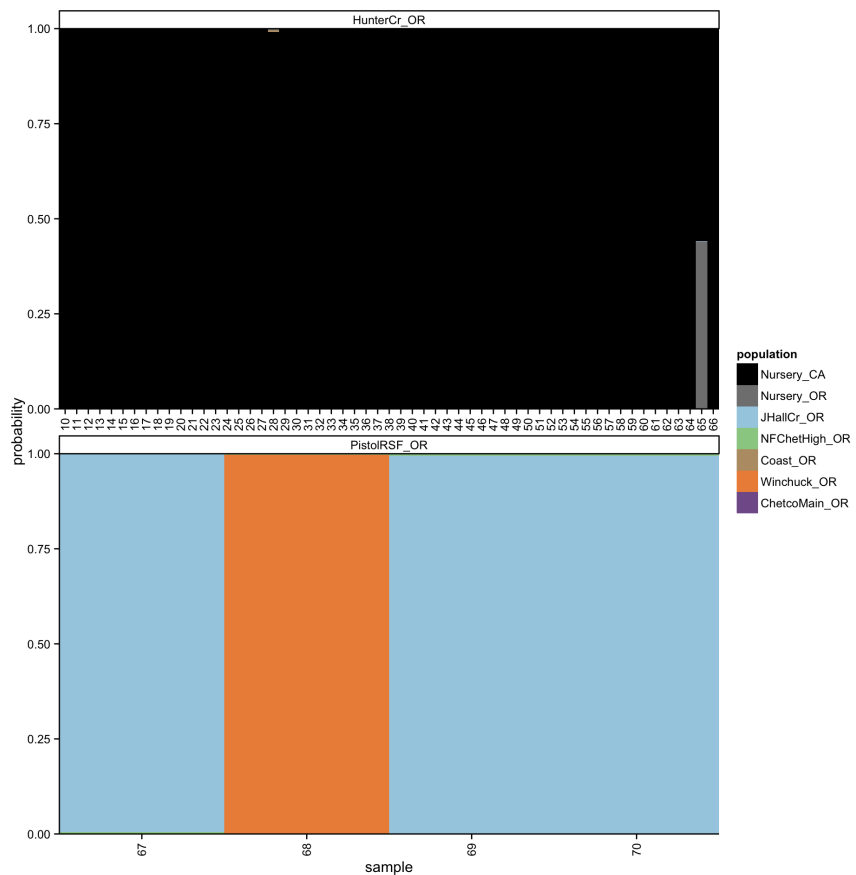


Figure 4.13: Graphical representation of predicted membership of *P. ramorum* isolates from Hunter Creek and Pistol River South Fork in forest and nursery populations. Each column represents a different isolate. Colors within the columns represent membership probabilities from the populations indicated in the legend.

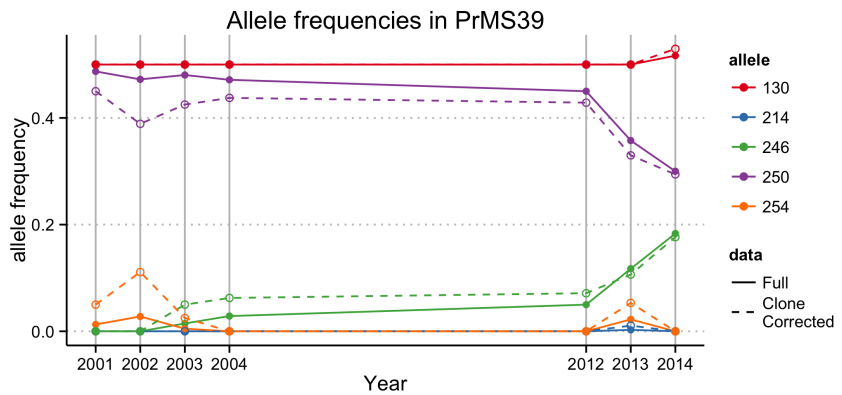


Figure 4.14: Allele frequencies of locus PrMS39 of *P. ramorum* across years of the forest populations. Years 2005 through 2011 have been omitted due to small sample sizes and outlier genotypes.

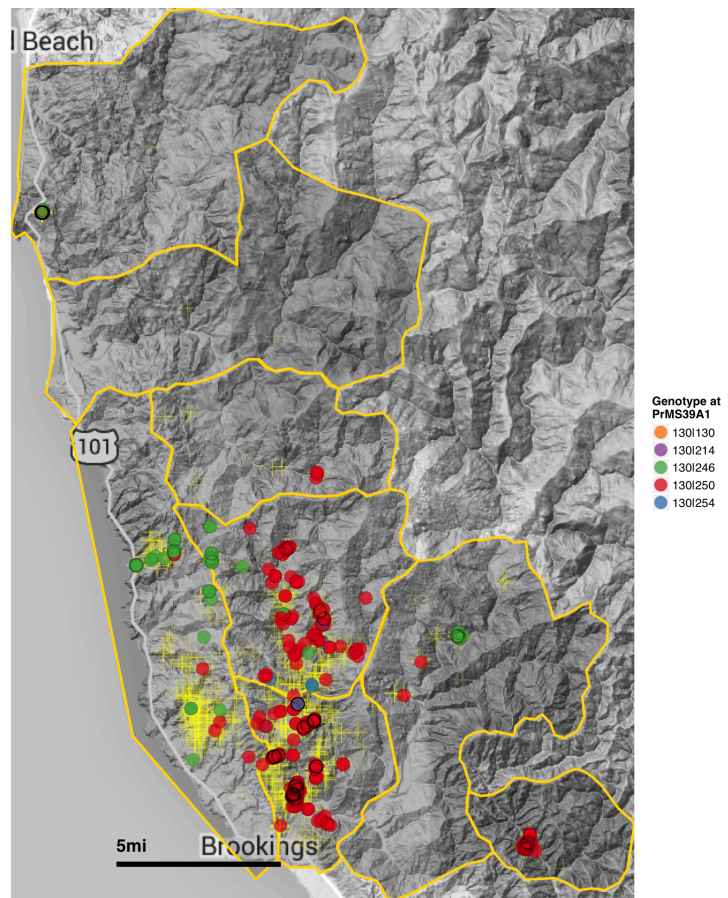


Figure 4.15: Map of the infected area in Curry county showing the *P. ramorum* genotypes at locus PrMS39. Each colored circle represents a different forest isolate while each yellow cross represents a sampled tree. Yellow borders denote different regions.

## Chapter 5: [Tentative Title] Population Dynamics of the Plant Pathogen *Phytophthora syringae* in Oregon Nurseries

### 5.1 Abstract

### 5.2 Introduction

*Phytophthora syringae* is the most important species affecting ornamentals produced in the Pacific Northwest. Recent nursery sampling efforts, aimed at characterizing the diversity of *Phytophthoras* within Oregon nurseries, have revealed the species *P. syringae* to be among the most abundant taxa found in the nurseries surveyed (Parke et al., 2014). *P. syringae* is adapted to cold weather and grows best in the cool, wet fall, winter and spring and is least active in summer (Erwin et al., 1996). Like *P. ramorum*, it has a wide host range including *Rhododendron*, *Camellia*, *Malus*, and many other taxa. It has the capability for outcrossing, self-fertilizing, and reproducing clonally. This pathogen has been found globally since 1881 and is problematic on woody ornamentals such as crabapple (*Malus spp.*), as it causes unsightly cankers that make the plant unsellable (Erwin et al., 1996). While the ecology of this pathogen has been studied to some degree, very little is known about the demographic history and population structure on a local and global scale.

Chapter 6: [Tentative Title] The Effect of Population Dynamics, Sample Size, and Marker Choice on the Index of Association

Zhian N. Kamvar and Niklaus J. Grünwald

Target Journal: **Molecular Ecology**

## 6.1 Abstract

TBD...

## 6.2 Introduction

Population genetics largely is based off of the neutral assumption that populations exist in Hardy-Weinberg Equilibrium (HWE) in that they are infinitely large, with no migration, no mutation, and randomly mating, where alleles across loci are I.I.D. This neutral model works well to describe populations that reproduce exclusively via sexual reproduction, but it becomes less useful when considering populations that undergo some form of clonal reproduction since the alleles for different samples are no longer I.I.D. This confounds the ability to accurately assess population demographics including effective population size (Orive, 1993). Many clonal organisms are also pathogenic, and knowing basic population dynamics of these pathogens is important for management strategies (de Meeûs et al., 2006; Milgroom, 1996; Milgroom and Fry, 1997; Nieuwenhuis and James, 2016; Smith et al., 1993).

The theory of population genetics for clonal organisms has been deeply investigated over time (Arnaud-Hanod et al., 2007; Halkett et al., 2005; Orive, 1993). In particular, there has been a re-occurring question of how much sex can be detected in a population of organisms with (partially) clonal reproduction (Ali et al., 2016; Balloux et al., 2003; de Meeûs and Balloux, 2004; Nieuwenhuis and James, 2016; Smith et al., 1993). For populations with well-defined sexual and clonal phases occurring at separate times, methods like *CloNcaSe* are effective for estimating the rate of sexual reproduction and

effective population size (Ali et al., 2016). However, when sexual reproduction is not a cyclical phenomena, this estimator is useless. Currently, a method commonly used to assess clonal reproduction is the index of association ( $I_A$ ), and its standardized version,  $\bar{r}_d$ , which measure multilocus linkage disequilibrium (Agapow and Burt, 2001; Brown et al., 1980; de Meeûs and Balloux, 2004; Haubold et al., 1998; Kamvar et al., 2014b; Smith et al., 1993). The value of  $I_A$  is measured as the ratio of observed variance in genetic distance between samples ( $V_O$ ) and expected variance ( $V_E$ ) (equation (6.1)) (Agapow and Burt, 2001; Smith et al., 1993).

$$I_A = \frac{V_O}{V_E} - 1 \quad (6.1)$$

The expected variance is practically modeled as the sum of the variances over  $m$  loci:  $V_E = \sum^m var_j$  (Agapow and Burt, 2001; Haubold et al., 1998). If the differences between samples are randomly distributed, we can expect the value of  $I_A$  to be zero (Agapow and Burt, 2001; Smith et al., 1993). Under scenarios of non-random mating (e.g. population structure or clonal reproduction), the observed variance would be greater than the expected due to a bimodal distribution of distances, and  $I_A$  would be greater than zero (Agapow and Burt, 2001; Milgroom, 2015; Smith et al., 1993). Agapow and Burt (2001) noted that this metric does not have an upper limit and increases with the number of loci. To correct this, they developed  $\bar{r}_d$  (equation (6.2)), which has a similar structure to a correlation coefficient and ranges from 0 (no linkage) to 1 (complete linkage).

$$\begin{aligned}\bar{r}_d &= \frac{\sum \sum cov_{j,k}}{\sum \sum \sqrt{var_j \cdot var_k}} \\ &= \frac{V_O - V_E}{2 \sum \sum \sqrt{var_j \cdot var_k}}\end{aligned}\tag{6.2}$$

Smith et al. (1993) demonstrated that  $I_A$  has the ability to detect non-random mating due to population structure, strict clonal reproduction, or a recent epidemic, but at that time, no one had quantified how much clonal reproduction had to occur to produce a significant value of  $I_A$ . This was of significant concern, considering that, as with any summary statistic, a lot of information is lost when evaluating a population based on  $I_A$  (Brown et al., 1980). One way to assess the effect of different population genetic scenarios was via simulations.

The effect of increasing levels of sexual reproduction on  $\bar{r}_d$  was investigated by de Meeûs and Balloux (2004) (noted in their publication as  $\bar{r}_D$ ). It was found that the mean value of  $\bar{r}_d$  decreased rapidly with relatively low levels of sexual reproduction, with large variances at low levels of sexual reproduction. This indicates that  $\bar{r}_d$  alone might not be well suited as a measure of clonal reproduction. The effect of sampling design on  $\bar{r}_d$  was tested by Prugnolle and de Meeûs (2010), finding that the value of  $\bar{r}_d$  is drastically reduced when clones from multiple populations are sampled, which can lead to an over-estimation of the level of recombination.

These studies laid the groundwork for understanding the behavior of  $\bar{r}_d$  under different scenarios of non-random mating in diploid organisms, but there were some limitations in available technology that prevented deep analysis from being performed.

For both studies, the only software available to analyze  $\bar{r}_d$  for diploid organisms was MULTILOCUS, which could only take one data set at a time (Agapow and Burt, 2001; de Meeûs and Balloux, 2004; Kamvar et al., 2014b; Prugnolle and de Meeûs, 2010). This constrained the researchers to only analyze a minimal set of populations (20) per scenario.

Since the distribution of  $I_A$  and  $\bar{r}_d$  are not known, the safest way to test for significance were random permutation tests that effectively created unlinked populations by shuffling individuals at each locus, independently and re-calculating  $I_A$  and  $\bar{r}_d$  (Agapow and Burt, 2001; Haubold et al., 1998; Smith et al., 1993). A one-sided *t*-test of significance was then used to see if the observed statistic was greater than the observed distribution.

While significance testing was available in MULTILOCUS in the form of random permutations, it was computationally expensive, and the analytical approach was only available in a software for haploid organisms (Agapow and Burt, 2001; Haubold and Hudson, 2000; Haubold et al., 1998; Kamvar et al., 2014b). As a result, power analysis of  $\bar{r}_d$  to detect clonal reproduction is still yet to be performed (de Meeûs and Balloux, 2004).

Since these studies came out, reduced-representation, high-throughput sequencing methods such as Genotyping-By-Sequencing (GBS) and RAD-seq have rapidly become popular tools for population genetic analysis (Davey and Blaxter, 2010; Davey et al., 2011; Elshire et al., 2011). These methods have the capability to generate thousands of unlinked markers at a fraction of the cost and time necessary to develop high quality microsatellite markers. These marker systems are also prone to high error rates

(Mastretta-Yanes et al., 2014). The index of association was developed for multiple loci in a time when obtaining even 100 unlinked markers posed a significant challenge. With the advent of these current technologies, how does marker choice and genotyping error affect the index of association?

Our current study aims to fill in the gaps left by the technical limitations of previous studies. In 2014, we developed the R package *poppr* for analysis of clonal populations, removing the limitations of data input and computational expense of analyzing the index of association, and in 2015, we expanded this to analysis of genome-wide SNP data (Kamvar et al., 2015b, 2014b; R Core Team, 2016). With these tools we set expand on previous studies by asking how sample size, marker choice, and clone-correction affect our ability to detect clonal reproduction in diploid populations. Our objectives to answer these questions are to (1) Re-analyze  $\bar{r}_d$  against increasing rates of sexual reproduction and different levels of population mixture in both microsatellite and SNP data sets. (2) Perform a power analysis of  $\bar{r}_d$ . (3) Assess how genotypic and allelic evenness and diversity affects  $\bar{r}_d$ . Because studies have observed significantly negative values of the  $I_A$  and  $\bar{r}_d$  ( $p \geq 0.95$ ), we additionally seek to characterize these populations to find common patterns that would indicate clonal or sexual reproduction.

### 6.3 Methods

Initial sets of simulations were created for different levels of sexual reproduction for each marker type. All simulations were performed with the python package simuPOP version 1.1.7 in python version 3.4. For each scenario, 100 simulations with 10 repli-

cates were created with a census size of 10,000 diploid individuals with equal mating type proportions evolved over 10,000 generations. From each replicate, 10, 25, 50, and 100 individuals were sampled without replacement for downstream analysis in R version 3.2 with the package *poppr* version 2.2.1 on full and clone-corrected data sets. All downstream analyses were run on the OSU CGRB Core Computing Facility (supplementary information).

### 6.3.1 Simulating Microsatellite Loci

Each population was simulated with 20 co-dominant, unlinked loci containing 6 to 10 alleles per locus with frequencies drawn from a uniform distribution and subsequently normalized. Before mating, mutations occurred at each locus at a rate of 1e-5 mutations/generation in a stepwise manner using the `StepwiseMutator()` operator.

### 6.3.2 GBS Simulations

Simulations of 10,000 binary loci spread evenly over 10 chromosomal fragments were simulated with a mutation rate of 1e-5 mutations per generation for forward and backward mutations using the `SNPMutator()` operator and a recombination rate of 1e-5 between adjacent loci using the `Recombinator()` operator.

### 6.3.3 Sexual Reproduction

Simulations of sexual reproduction were analyzed at 10 rates of sexual reproduction on a log scale (0.0, 1e-4, 5e-4, 1e-3, 5e-3, 1e-2, 5e-2, 0.1, 0.5, 1.0) reflecting the fraction of individuals in generation  $t+1$  produced via sexual reproduction. One to three offspring could be produced at each mating event. For sexual events, two parents were chosen randomly from the population with the `RandomSelection()` operator and offspring genotypes were created via the `MendelianGenoTransmitter()` operator. The clonal fraction was created by randomly sampling individuals from the population and duplicating their genotypes with the `CloneGenoTransmitter()` operator. If one mating type was lost before 10,000 generations, the simulation would continue to completion with only clonal reproduction.

### 6.3.4 Analysis of Microsatellite Data

The standardized index of association ( $\bar{r}_d$ ) was calculated for full and clone-corrected data using the *poppr* function `ia()`. Tests for significance were performed by randomly permuting the alleles at each locus independently and then assessing  $\bar{r}_d$ . This was done 999 times for each replicate population. Re-sampling was not performed with clone-corrected data. The p-values reflect the proportion of observations greater than the observed statistic. Estimates of genotypic diversity were assessed with the *poppr* function `diversity_boot()` with 999 bootstrap replicates, recording the estimate and variance.

### 6.3.5 Analysis of SNP Data

Because GBS data are associated with high error rates, we additionally wanted to assess the effect of error and missing data on analysis. To do this, we used scripts written for Kamvar et al. (2015b) to randomly insert missing data (via the `pop_NA()` function) and genotyping errors (via the `pop_mutator()`) (Kamvar et al., 2015a) at rates of 5% and 10% each. We then used the *poppr* function `mlg.filter()` to with the farthest neighbor algorithm to collapse multilocus genotypes with 5% and 10% similarity and compared the results with the known genotypes. Genotypic diversity was assessed with the *poppr* function `diversity_boot()` with 999 bootstrap replicates on the filtered data sets, recording the variance.

The overall value of  $\bar{r}_d$  was calculated for each simulation with the *poppr* function `bitwise.ia()`. To assess within-chromosome dynamics, values of  $\bar{r}_d$  were calculated along chromosomes using the *poppr* function `win.ia()` along windows of 50 and 100 SNPs. Cross-chromosome dynamics of  $\bar{r}_d$  were assessed by utilizing random samples of 50, 100, and 1000 SNPs replicated 999 times for each population sample.

### 6.3.6 Power Analysis

The Receiver Operating Characteristic (ROC) curve is a method of assessing the explanatory power of a method by assessing the true positive fraction of tests to a false positive fraction (Metz, 1978). Briefly, if a method has perfect explanatory power, the area under the ROC curve will be equal to 1. If a method has no explanatory power, the area under the ROC curve will be equal to 0.5. ROC analysis was carried

as described in Metz (1978) as a comparison of the false positive fraction to the true positive fraction as you increase the level of rejection, ( $\alpha$ ). The null hypothesis for the ROC analysis was defined where the rate of sexual reproduction was 100%. All other rates were considered to be separate alternative hypotheses. The curves were calculated by analyzing the data sets over increasing values of  $\alpha$  from 0 to 1 in increments of 0.01. The area under the ROC curves was calculated using the `trapz()` function in the R package *pracma* version 1.9.5 (Borchers, 2016). ANOVA was run with the following models:

---

False Positive Rate ~ Sex Rate + Sample Size

---

Area Under ROC Curve ~ Sex Rate + Sample Size

---

## Bibliography

- Agapow, P.-M., and Burt, A. (2001). Indices of multilocus linkage disequilibrium. *Molecular Ecology Notes* 1, 101–102. doi:[10.1046/j.1471-8278.2000.00014.x](https://doi.org/10.1046/j.1471-8278.2000.00014.x).
- Ali, S., Soubeyrand, S., Gladieux, P., Giraud, T., Leconte, M., Gautier, A., et al. (2016). Cloncase: Estimation of sex frequency and effective population size by clonemate resampling in partially clonal organisms. *Molecular Ecology Resources*. doi:[10.1111/1755-0998.12511](https://doi.org/10.1111/1755-0998.12511).
- Anderson, J. B., and Kohn, L. M. (1995). Clonality in soilborne, plant-pathogenic fungi. *Annual review of phytopathology* 33, 369–391.
- Arnaud-Hanod, S., Duarte, C. M., Alberto, F., and Serrão, E. A. (2007). Standardizing methods to address clonality in population studies. *Molecular Ecology* 16, 5115–5139. doi:[10.1111/j.1365-294X.2007.03535.x](https://doi.org/10.1111/j.1365-294X.2007.03535.x).
- Baldauf, S. (2003). The deep roots of eukaryotes. *Science* 300, 1703–1706. doi:[10.1126/science.1085544](https://doi.org/10.1126/science.1085544).
- Balloux, F., Lehmann, L., and de Meeûs, T. (2003). The population genetics of clonal and partially clonal diploids. *Genetics* 164, 1635–1644.
- Bivand, R., Keitt, T., and Rowlingson, B. (2014). *rgdal: Bindings for the Geospatial Data Abstraction Library*. Available at: <https://CRAN.R-project.org/package=rgdal>.
- Borchers, H. W. (2016). *Pracma: Practical numerical math functions*. Available at: <https://CRAN.R-project.org/package=pracma>.
- Brown, A., Feldman, M., and Nevo, E. (1980). Multilocus structure of natural populations of *Hordeum spontaneum*. *Genetics* 96, 523–536. Available at: <http://www.genetics.org/content/96/2/523.abstract>.
- Brownstein, M. J., Carpten, J. D., and Smith, J. R. (1996). Modulation of non-templated nucleotide addition by Taq DNA polymerase: primer modifications that

- facilitate genotyping. *BioTechniques* 20, 1004–6, 1008–10.
- Bruvo, R., Michiels, N. K., D'Souza, T. G., and Schulenburg, H. (2004). A simple method for the calculation of microsatellite genotype distances irrespective of ploidy level. *Molecular Ecology* 13, 2101–2106.
- Butlin, R. K. (2000). Virgin rotifers. *Trends in Ecology & Evolution* 15, 389–390. doi:[10.1016/S0169-5347\(00\)01937-6](https://doi.org/10.1016/S0169-5347(00)01937-6).
- Canty, A., and Ripley, B. D. (2015). *Boot: Bootstrap r (s-plus) functions*. Available at: <https://CRAN.R-project.org/package=boot>.
- Chakarov, N., Linke, B., Boerner, M., Goesmann, A., Krüger, O., and Hoffman, J. I. (2015). Apparent vector-mediated parent-to-offspring transmission in an avian malaria-like parasite. *Molecular ecology* 24, 1355–1363.
- Cooke, D. E., Cano, L. M., Raffaele, S., Bain, R. A., Cooke, L. R., Etherington, G. J., et al. (2012). Genome analyses of an aggressive and invasive lineage of the Irish potato famine pathogen. *PLoS pathogens* 8, e1002940.
- Croucher, P. J. P., Mascheretti, S., and Garbelotto, M. (2013). Combining field epidemiological information and genetic data to comprehensively reconstruct the invasion history and the microevolution of the sudden oak death agent *Phytophthora ramorum* (Stramenopila: Oomycetes) in California. *Biological Invasions* 15, 2281–2297. doi:[10.1007/s10530-013-0453-8](https://doi.org/10.1007/s10530-013-0453-8).
- Csardi, G., and Nepusz, T. (2006). The igraph software package for complex network research. *InterJournal Complex Systems*, 1695. Available at: <http://igraph.org>.
- Dagum, L., and Menon, R. (1998). OpenMP: An industry standard API for shared-memory programming. *Computational Science & Engineering, IEEE* 5, 46–55.
- Davey, J. W., and Blaxter, M. L. (2010). RADSeq: next-generation population genetics. *Briefings in Functional Genomics* 9, 416–423. doi:[10.1093/bfgp/elq031](https://doi.org/10.1093/bfgp/elq031).
- Davey, J. W., Hohenlohe, P. A., Etter, P. D., Boone, J. Q., Catchen, J. M., and Blaxter, M. L. (2011). Genome-wide genetic marker discovery and genotyping using next-generation sequencing. *Nature Reviews Genetics* 12, 499–510. doi:[10.1038/nrg3012](https://doi.org/10.1038/nrg3012).
- de Meeûs, T., and Balloux, F. (2004). Clonal reproduction and linkage disequilibrium in diploids: A simulation study. *Infection, Genetics and Evolution* 4, 345–351.

doi:[10.1016/j.meegid.2004.05.002](https://doi.org/10.1016/j.meegid.2004.05.002).

de Meeûs, T., Lehmann, L., and Balloux, F. (2006). Molecular epidemiology of clonal diploids: a quick overview and a short DIY (do it yourself) notice. *Infection, Genetics and Evolution* 6, 163–170. doi:[10.1016/j.meegid.2005.02.004](https://doi.org/10.1016/j.meegid.2005.02.004).

Dobzhansky, T. (1973). Nothing in biology makes sense except in the light of evolution. *The American Biology Teacher* 75, 87–91.

Dray, S., and Dufour, A.-B. (2007). The ade4 package: Implementing the duality diagram for ecologists. *Journal of Statistical Software* 22. doi:[10.18637/jss.v022.i04](https://doi.org/10.18637/jss.v022.i04).

Elshire, R. J., Glaubitz, J. C., Sun, Q., Poland, J. A., Kawamoto, K., Buckler, E. S., et al. (2011). A robust, simple genotyping-by-sequencing (GBS) approach for high diversity species. *PLoS ONE* 6, e19379. doi:[10.1371/journal.pone.0019379](https://doi.org/10.1371/journal.pone.0019379).

Erwin, D. C., Ribeiro, O. K., and others (1996). *Phytophthora diseases worldwide*. St. Paul, Minnesota, USA: American Phytopathological Society (APS Press).

Everhart, S. E., and Scherm, H. (2015). Fine-scale genetic structure of *Monilinia fructicola* during brown rot epidemics within individual peach tree canopies. *Phytopathology* 105, 542–549. doi:[10.1094/phyto-03-14-0088-r](https://doi.org/10.1094/phyto-03-14-0088-r).

Everhart, S. E., Tabima, J. F., and Grünwald, N. J. (2014). “*Phytophthora ramorum*,” in *Genomics of plant-associated fungi and oomycetes: Dicot pathogens* (Berlin, Heidelberg: Springer), 159–174. doi:[10.1007/978-3-662-44056-8\\_8](https://doi.org/10.1007/978-3-662-44056-8_8).

Excoffier, L., Smouse, P. E., and Quattro, J. M. (1992). Analysis of molecular variance inferred from metric distances among DNA haplotypes: Application to human mitochondrial DNA restriction data. *Genetics* 131, 479–91.

Eyre, C. A., Kozanitas, M., and Garbelotto, M. (2013). Population Dynamics of Aerial and Terrestrial Populations of *Phytophthora ramorum* in a California Forest Under Different Climatic Conditions. *Phytopathology* 103, 1141–1152. doi:[10.1094/phyto-11-12-0290-r](https://doi.org/10.1094/phyto-11-12-0290-r).

Falush, D., Stephens, M., and Pritchard, J. K. (2003). Inference of population structure using multilocus genotype data: Linked loci and correlated allele frequencies. *Genetics* 164, 1567–1587. Available at: <http://www.genetics.org/content/164/4/1567.abstract>.

Goss, E. M., Larsen, M., Chastagner, G. A., Givens, D. R., and Grünwald, N. J. (2009).

- Population genetic analysis infers migration pathways of *Phytophthora ramorum* in US nurseries. *PLoS Pathog* 5, e1000583. doi:[10.1371/journal.ppat.1000583](https://doi.org/10.1371/journal.ppat.1000583).
- Goss, E. M., Larsen, M., Vercauteren, A., Werres, S., Heungens, K., and Grünwald, N. J. (2011). *Phytophthora ramorum* in Canada: Evidence for Migration Within North America and from Europe. *Phytopathology* 101, 166–171. doi:[10.1094/phyto-05-10-0133](https://doi.org/10.1094/phyto-05-10-0133).
- Goss, E. M., Tabima, J. F., Cooke, D. E., Restrepo, S., Fry, W. E., Forbes, G. A., et al. (2014). The Irish potato famine pathogen *Phytophthora infestans* originated in central Mexico rather than the Andes. *Proceedings of the National Academy of Sciences* 111, 8791–8796.
- Goudet, J. (2005). Hierfstat, a package for R to compute and test hierarchical F-statistics. *Molecular Ecology Notes* 5, 184–186.
- Gross, A., Hosoya, T., and Queloz, V. (2014). Population structure of the invasive forest pathogen *Hymenoscyphus pseudoalbidus*. *Molecular ecology* 23, 2943–2960.
- Grünwald, N. J., and Goss, E. M. (2011). Evolution and Population Genetics of Exotic and Re-Emerging Pathogens: Novel Tools and Approaches. *Annu. Rev. Phytopathol.* 49, 249–267. doi:[10.1146/annurev-phyto-072910-095246](https://doi.org/10.1146/annurev-phyto-072910-095246).
- Grünwald, N. J., and Hoheisel, G.-A. (2006). Hierarchical analysis of diversity, selfing, and genetic differentiation in populations of the oomycete *Aphanomyces euteiches*. *Phytopathology* 96, 1134–1141.
- Grünwald, N. J., Garbelotto, M., Goss, E. M., Heungens, K., and Prospero, S. (2012). Emergence of the sudden oak death pathogen *Phytophthora ramorum*. *Trends in Microbiology* 20, 131–138. doi:[10.1016/j.tim.2011.12.006](https://doi.org/10.1016/j.tim.2011.12.006).
- Grünwald, N. J., Goodwin, S. B., Milgroom, M. G., and Fry, W. E. (2003). Analysis of Genotypic Diversity Data for Populations of Microorganisms. *Phytopathology* 93, 738–746. doi:[10.1094/phyto.2003.93.6.738](https://doi.org/10.1094/phyto.2003.93.6.738).
- Grünwald, N. J., Goss, E. M., and Press, C. M. (2008a). *Phytophthora ramorum*: a pathogen with a remarkably wide host range causing sudden oak death on oaks and ramorum blight on woody ornamentals. *Molecular Plant Pathology* 9, 729–740. doi:[10.1111/j.1364-3703.2008.00500.x](https://doi.org/10.1111/j.1364-3703.2008.00500.x).
- Grünwald, N. J., Goss, E. M., Ivors, K., Garbelotto, M., Martin, F. N., Prospero, S., et al. (2009). Standardizing the Nomenclature for Clonal Lineages of the

- Sudden Oak Death Pathogen, *Phytophthora ramorum*. *Phytopathology* 99, 792–795. doi:[10.1094/phyto-99-7-0792](https://doi.org/10.1094/phyto-99-7-0792).
- Grünwald, N. J., Kitner, M., McDonald, V., and Goss, E. M. (2008b). Susceptibility in *Viburnum* to *Phytophthora ramorum*. *Plant Disease* 92, 210–214. doi:[10.1094/pdis-92-2-0210](https://doi.org/10.1094/pdis-92-2-0210).
- Grünwald, N. J., Martin, F. N., Larsen, M. M., Sullivan, C. M., Press, C. M., Coffey, M. D., et al. (2011). Phytophthora-ID.org: a sequence-based *Phytophthora* identification tool. *Plant Disease* 95, 337–342.
- Haas, B. J., Kamoun, S., Zody, M. C., Jiang, R. H., Handsaker, R. E., Cano, L. M., et al. (2009). Genome sequence and analysis of the Irish potato famine pathogen *Phytophthora infestans*. *Nature* 461, 393–398. doi:[10.1038/nature08358](https://doi.org/10.1038/nature08358).
- Halkett, F., Simon, J., and Balloux, F. (2005). Tackling the population genetics of clonal and partially clonal organisms. *Trends in Ecology & Evolution* 20, 194–201. doi:[10.1016/j.tree.2005.01.001](https://doi.org/10.1016/j.tree.2005.01.001).
- Hansen, E. M., Kanaskie, A., Prospero, S., McWilliams, M., Goheen, E. M., Osterbauer, N., et al. (2008). Epidemiology of *Phytophthora ramorum* in Oregon tanoak forests. *Canadian Journal of Forest Research* 38, 1133–1143. doi:[10.1139/x07-217](https://doi.org/10.1139/x07-217).
- Haubold, B., and Hudson, R. R. (2000). LIAN 3.0: Detecting linkage disequilibrium in multilocus data. *Bioinformatics* 16, 847–849. doi:[10.1093/bioinformatics/16.9.847](https://doi.org/10.1093/bioinformatics/16.9.847).
- Haubold, B., Travisano, M., Rainey, P. B., and Hudson, R. R. (1998). Detecting linkage disequilibrium in bacterial populations. *Genetics* 150, 1341–8.
- Heck, K. L., van Belle, G., and Simberloff, D. (1975). Explicit calculation of the rarefaction diversity measurement and the determination of sufficient sample size. *Ecology* 56, 1459–1461. doi:[10.2307/1934716](https://doi.org/10.2307/1934716).
- Hurlbert, S. H. (1971). The nonconcept of species diversity: A critique and alternative parameters. *Ecology* 52, 577–586. doi:[10.2307/1934145](https://doi.org/10.2307/1934145).
- Ivors, K., Garbelotto, M., Vries, I. D. E., Ruyter-spira, C., Hekkert, B. T., Rosenzweig, N., et al. (2006). Microsatellite markers identify three lineages of *Phytophthora ramorum* in US nurseries, yet single lineages in US forest and European nursery populations. *Molecular Ecology* 15, 1493–1505. doi:[10.1111/j.1365-294x.2006.02864.x](https://doi.org/10.1111/j.1365-294x.2006.02864.x).
- Jombart, T. (2008). Adegenet: a R package for the multivariate analysis of genetic

- markers. *Bioinformatics* 24, 1403–1405. doi:[10.1093/bioinformatics/btn129](https://doi.org/10.1093/bioinformatics/btn129).
- Jombart, T., and Ahmed, I. (2011). Adegenet 1.3-1: New tools for the analysis of genome-wide SNP data. *Bioinformatics* 27, 3070–3071.
- Jombart, T., Devillard, S., and Balloux, F. (2010). Discriminant analysis of principal components: A new method for the analysis of genetically structured populations. *BMC Genet* 11, 94. doi:[10.1186/1471-2156-11-94](https://doi.org/10.1186/1471-2156-11-94).
- Kahle, D., and Wickham, H. (2013). ggmap: Spatial Visualization with ggplot2. *The R Journal* 5, 144–161. Available at: <http://journal.r-project.org/archive/2013-1/kahle-wickham.pdf>.
- Kamoun, S., Furzer, O., Jones, J. D. G., Judelson, H. S., Ali, G. S., Dalio, R. J. D., et al. (2014). The top 10 oomycete pathogens in molecular plant pathology. *Molecular Plant Pathology* 16, 413–434. doi:[10.1111/mpp.12190](https://doi.org/10.1111/mpp.12190).
- Kamvar, Z. N., Brooks, J. C., and Grunwald, N. J. (2015a). Supplementary Material for Frontiers Plant Genetics and Genomics 'Novel R tools for analysis of genome-wide population genetic data with emphasis on clonality'. doi:[10.5281/zenodo.17424](https://doi.org/10.5281/zenodo.17424).
- Kamvar, Z. N., Brooks, J. C., and Grünwald, N. J. (2015b). Novel R tools for analysis of genome-wide population genetic data with emphasis on clonality. *Frontiers in Genetics* 6. doi:[10.3389/fgene.2015.00208](https://doi.org/10.3389/fgene.2015.00208).
- Kamvar, Z. N., Larsen, M. M., Kanaskie, A. M., Hansen, E. M., and Grünwald, N. J. (2014a). Sudden\_Oak\_Death\_in\_Oregon\_Forests: Spatial and temporal population dynamics of the sudden oak death epidemic in Oregon Forests. doi:[10.5281/zenodo.13007](https://doi.org/10.5281/zenodo.13007).
- Kamvar, Z. N., Larsen, M. M., Kanaskie, A. M., Hansen, E. M., and Grünwald, N. J. (2015c). Spatial and temporal analysis of populations of the sudden oak death pathogen in oregon forests. *Phytopathology* 105, 982–989. doi:[10.1094/phyto-12-14-0350-fi](https://doi.org/10.1094/phyto-12-14-0350-fi).
- Kamvar, Z. N., Tabima, J. F., and Grünwald, N. J. (2014b). Poppr : an R package for genetic analysis of populations with clonal, partially clonal, and/or sexual reproduction. *PeerJ* 2, e281. doi:[10.7717/peerj.281](https://doi.org/10.7717/peerj.281).
- Kroon, L. P., Brouwer, H., Cock, A. W. de, and Govers, F. (2012). The Genus

- Phytophthora*. *Phytopathology* 102, 348–364. doi:[10.1094/PHYTO-01-11-0025](https://doi.org/10.1094/PHYTO-01-11-0025).
- Laloë, D., Jombart, T., Dufour, A.-B., and Moazami-Goudarzi, K. (2007). Consensus genetic structuring and typological value of markers using multiple co-inertia analysis. *Genetics Selection Evolution* 39, 1–23.
- Lees, A., Wattier, R., Shaw, D., Sullivan, L., Williams, N., and Cooke, D. (2006). Novel microsatellite markers for the analysis of *Phytophthora infestans* populations. *Plant Pathology* 55, 311–319.
- Li, Y., Cooke, D. E., Jacobsen, E., and Lee, T. van der (2013). Efficient multiplex simple sequence repeat genotyping of the oomycete plant pathogen *Phytophthora infestans*. *Journal of microbiological methods* 92, 316–322.
- Linde, C., Zhan, J., and McDonald, B. (2002). Population structure of *Mycosphaerella graminicola*: From lesions to continents. *Phytopathology* 92, 946–955.
- Ludwig, J. A., and Reynolds, J. F. (1988). *Statistical ecology: A primer in methods and computing*. John Wiley & Sons.
- Luikart, G., England, P. R., Tallmon, D., Jordan, S., and Taberlet, P. (2003). The power and promise of population genomics: From genotyping to genome typing. *Nature Reviews Genetics* 4, 981–994.
- Mantel, N. (1967). The detection of disease clustering and a generalized regression approach. *Cancer research* 27, 209–220.
- Mascheretti, S., Croucher, P. J. P., Kozanitas, M., Baker, L., and Garbelotto, M. (2009). Genetic epidemiology of the Sudden Oak Death pathogen *Phytophthora ramorum* in California. *Molecular Ecology* 18, 4577–4590. doi:[10.1111/j.1365-294x.2009.04379.x](https://doi.org/10.1111/j.1365-294x.2009.04379.x).
- Mascheretti, S., Croucher, P. J. P., Vettraino, A., Prospero, S., and Garbelotto, M. (2008). Reconstruction of the Sudden Oak Death epidemic in California through microsatellite analysis of the pathogen *Phytophthora ramorum*. *Molecular Ecology* 17, 2755–2768. doi:[10.1111/j.1365-294x.2008.03773.x](https://doi.org/10.1111/j.1365-294x.2008.03773.x).
- Mastretta-Yanes, A., Arrigo, N., Alvarez, N., Jorgensen, T. H., Piñero, D., and Emerson, B. C. (2014). Restriction site-associated DNA sequencing, genotyping error estimation and *de novo* assembly optimization for population genetic inference.

- Molecular Ecology Resources* 15, 28–41. doi:[10.1111/1755-0998.12291](https://doi.org/10.1111/1755-0998.12291).
- McDonald, B. A., and Linde, C. (2002). The population genetics of plant pathogens and breeding strategies for durable resistance. *Euphytica* 124, 163–180. doi:[10.1023/A:1015678432355](https://doi.org/10.1023/A:1015678432355).
- Meirmans, P. G., and Van Tienderen, P. H. (2004). GENOTYPE and GENODIVE: Two programs for the analysis of genetic diversity of asexual organisms. *Molecular Ecology Notes* 4, 792–794.
- Metz, C. E. (1978). Basic principles of ROC analysis. in *Seminars in nuclear medicine* (Elsevier), 283–298. doi:[10.1016/S0001-2998\(78\)80014-2](https://doi.org/10.1016/S0001-2998(78)80014-2).
- Metzger, M. J., Reinisch, C., Sherry, J., and Goff, S. P. (2015). Horizontal transmission of clonal cancer cells causes leukemia in soft-shell clams. *Cell* 161, 255–263.
- Michalakis, Y., and Excoffier, L. (1996). A generic estimation of population subdivision using distances between alleles with special reference for microsatellite loci. *Genetics* 142, 1061–1064.
- Milgroom, M. G. (1996). Recombination and the multilocus structure of fungal populations. *Annual review of phytopathology* 34, 457–477.
- Milgroom, M. G. (2015). *Population biology of plant pathogens: Genetics, ecology, and evolution*. 3340 Pilot Knob Road, St. Paul, MN 55121, USA: APS Press.
- Milgroom, M. G., Levin, S. A., and Fry, W. E. (1989). Population genetics theory and fungicide resistance. *Plant disease epidemiology* 2, 340–367.
- Milgroom, M., and Fry, W. E. (1997). Contributions of population genetics to plant disease epidemiology and management. *Advances in Botanical Research* 24, 1–30. doi:[10.1016/S0065-2296\(08\)60069-5](https://doi.org/10.1016/S0065-2296(08)60069-5).
- Nei, M. (1973). Analysis of gene diversity in subdivided populations. *Proceedings of the National Academy of Sciences* 70, 3321–3323.
- Nieuwenhuis, B. P. S., and James, T. Y. (2016). The frequency of sex in fungi. *Philosophical Transactions of the Royal Society B: Biological Sciences* 371, 20150540. doi:[10.1098/rstb.2015.0540](https://doi.org/10.1098/rstb.2015.0540).
- Oksanen, J., Blanchet, F. G., Kindt, R., Legendre, P., Minchin, P. R., O'Hara, R. B., et al. (2013). *Vegan: Community ecology package*. Available at: <https://CRAN.R-project.org/package=vegan>

[project.org/package=vegan](http://CRAN.R-project.org/package=vegan).

Oksanen, J., Blanchet, F. G., Kindt, R., Legendre, P., Minchin, P. R., O'Hara, R. B., et al. (2015). *Vegan: Community ecology package*. Available at: <http://CRAN.R-project.org/package=vegan>.

Orive, M. E. (1993). Effective population size in organisms with complex life-histories. *Theoretical Population Biology* 44, 316–340. doi:[10.1006/tpbi.1993.1031](https://doi.org/10.1006/tpbi.1993.1031).

Paradis, E., Claude, J., and Strimmer, K. (2004). APE: Analyses of phylogenetics and evolution in r language. *Bioinformatics* 20, 289–290. doi:[10.1093/bioinformatics/btg412](https://doi.org/10.1093/bioinformatics/btg412).

Parke, J. L., Knaus, B. J., Fieland, V. J., Lewis, C., and Grünwald, N. J. (2014). Phytophthora community structure analyses in Oregon nurseries inform systems approaches to disease management. *Phytopathology* 104, 1052–1062. doi:[10.1094/PHYTO-01-14-0014-R](https://doi.org/10.1094/PHYTO-01-14-0014-R).

Pielou, E. (1975). Ecological diversity.

Poucke, K. V., Franceschini, S., Webber, J. F., Vercauteren, A., Turner, J. A., McCracken, A. R., et al. (2012). Discovery of a fourth evolutionary lineage of *Phytophthora ramorum*: EU2. *Fungal Biology* 116, 1178–1191. doi:[10.1016/j.funbio.2012.09.003](https://doi.org/10.1016/j.funbio.2012.09.003).

Prevosti, A., Ocaña, J., and Alonso, G. (1975). Distances between populations of *Drosophila subobscura*, based on chromosome arrangement frequencies. *Theoretical and Applied Genetics* 45, 231–241.

Prospero, S., Black, J. A., and Winton, L. M. (2004). Isolation and characterization of microsatellite markers in *Phytophthora ramorum*, the causal agent of sudden oak death. *Molecular Ecology Notes* 4, 672–674. doi:[10.1111/j.1471-8286.2004.00778.x](https://doi.org/10.1111/j.1471-8286.2004.00778.x).

Prospero, S., Grünwald, N. J., Winton, L. M., and Hansen, E. M. (2009). Migration Patterns of the Emerging Plant Pathogen *Phytophthora ramorum* on the West Coast of the United States of America. *Phytopathology* 99, 739–749. doi:[10.1094/phyto-99-6-0739](https://doi.org/10.1094/phyto-99-6-0739).

Prospero, S., Hansen, E. M., Grünwald, N. J., and Winton, L. M. (2007). Population dynamics of the sudden oak death pathogen *Phytophthora ramorum* in Oregon from 2001 to 2004. *Molecular Ecology* 16, 2958–2973. doi:[10.1111/j.1365](https://doi.org/10.1111/j.1365)

[294x.2007.03343.x.](#)

Prugnolle, F., and de Meeûs, T. (2010). Apparent high recombination rates in clonal parasitic organisms due to inappropriate sampling design. *Heredity* 104, 135–140. doi:[10.1038/hdy.2009.128](https://doi.org/10.1038/hdy.2009.128).

R Core Team (2014). *R: A language and environment for statistical computing*. Vienna, Austria: R Foundation for Statistical Computing Available at: <https://www.R-project.org/>.

R Core Team (2015). *R: A language and environment for statistical computing*. Vienna, Austria: R Foundation for Statistical Computing Available at: <http://www.R-project.org/>.

R Core Team (2016). *R: A language and environment for statistical computing*. Vienna, Austria: R Foundation for Statistical Computing Available at: <https://www.R-project.org/>.

Rizzo, D. M., Garbelotto, M., and Hansen, E. M. (2005). *Phytophthora ramorum*: Integrative Research and Management of an Emerging Pathogen in California and Oregon Forests. *Annu. Rev. Phytopathol.* 43, 309–335. doi:[10.1146/annurev.phyto.42.040803.140418](https://doi.org/10.1146/annurev.phyto.42.040803.140418).

Rizzo, D. M., Garbelotto, M., Davidson, J. M., Slaughter, G. W., and Koike, S. T. (2002). *Phytophthora ramorum* as the Cause of Extensive Mortality of *Quercus* spp. and *Lithocarpus densiflorus* in California. *Plant Disease* 86, 205–214. doi:[10.1094/pdis.2002.86.3.205](https://doi.org/10.1094/pdis.2002.86.3.205).

Rosvall, M., and Bergstrom, C. T. (2008). Maps of random walks on complex networks reveal community structure. *Proceedings of the National Academy of Sciences* 105, 1118–1123.

Shannon, C. (2001). A mathematical theory of communication. *ACM SIGMOBILE Mobile Computing and Communications Review* 5, 3–55. Available at: <http://cm.bell-labs.com/cm/ms/what/shannonday/shannon1948.pdf>.

Smith, J. M., Smith, N. H., O'Rourke, M., and Spratt, B. G. (1993). How clonal are bacteria? *Proceedings of the National Academy of Sciences* 90, 4384–4388. doi:[10.1073/pnas.90.10.4384](https://doi.org/10.1073/pnas.90.10.4384).

Sokal, R. R. (1958). A statistical method for evaluating systematic relationships. *Univ*

- Kans Sci Bull* 38, 1409–1438.
- Stoddart, J. A., and Taylor, J. F. (1988). Genotypic diversity: Estimation and prediction in samples. *Genetics* 118, 705–11.
- Taylor, J. W., and Fisher, M. C. (2003). Fungal multilocus sequence typing – it's not just for bacteria. *Current opinion in microbiology* 6, 351–356.
- Tyler, B. M. (2007). *Phytophthora sojae*: root rot pathogen of soybean and model oomycete. *Molecular Plant Pathology* 8, 1–8. doi:[10.1111/j.1364-3703.2006.00373.x](https://doi.org/10.1111/j.1364-3703.2006.00373.x).
- Vercauteren, A., Dobbelaere, I. D., Grünwald, N. J., Bonants, P., Bockstaele, E. V., Maes, M., et al. (2010). Clonal expansion of the Belgian *Phytophthora ramorum* populations based on new microsatellite markers. *Molecular Ecology* 19, 92–107. doi:[10.1111/j.1365-294x.2009.04443.x](https://doi.org/10.1111/j.1365-294x.2009.04443.x).
- Vercauteren, A., Larsen, M., Goss, E., Grunwald, N. J., Maes, M., and Heungens, K. (2011). Identification of new polymorphic microsatellite markers in the NA1 and NA2 lineages of *Phytophthora ramorum*. *Mycologia* 103, 1245–1249. doi:[10.3852/10-420](https://doi.org/10.3852/10-420).
- Welch, D. B. M., and Meselson, M. (2000). Evidence for the evolution of bdelloid rotifers without sexual reproduction or genetic exchange. *Science* 288, 1211–1215. doi:[10.1126/science.288.5469.1211](https://doi.org/10.1126/science.288.5469.1211).
- Welch, D. B. M., and Meselson, M. S. (2001). Rates of nucleotide substitution in sexual and anciently asexual rotifers. *Proceedings of the National Academy of Sciences* 98, 6720–6724. doi:[10.1073/pnas.111144598](https://doi.org/10.1073/pnas.111144598).
- Werres, S., Marwitz, R., veld, W. A. M. I., Cock, A. W. D., Bonants, P. J., Weerdt, M. D., et al. (2001). *Phytophthora ramorum* sp. nov., a new pathogen on Rhododendron and Viburnum. *Mycological Research* 105, 1155–1165. doi:[10.1016/s0953-7562\(08\)61986-3](https://doi.org/10.1016/s0953-7562(08)61986-3).
- Wickham, H. (2009). *ggplot2: Elegant Graphics for Data Analysis*. Springer-Verlag New York Available at: <http://ggplot2.org>.
- Wickham, H., and Chang, W. (2015). *Devtools: Tools to make developing R packages easier*. Available at: <http://CRAN.R-project.org/package=devtools>.
- Winton, L. M., and Hansen, E. M. (2001). Molecular diagnosis of *Phytophthora*

*lateralis* in trees, water, and foliage baits using multiplex polymerase chain reaction. *Forest Pathol* 31, 275–283. doi:[10.1046/j.1439-0329.2001.00251.x](https://doi.org/10.1046/j.1439-0329.2001.00251.x).

Yoshida, K., Schuenemann, V. J., Cano, L. M., Pais, M., Mishra, B., Sharma, R., et al. (2013). The rise and fall of the *Phytophthora infestans* lineage that triggered the Irish potato famine. *eLife* 2, e00731. doi:[10.7554/eLife.00731.001](https://doi.org/10.7554/eLife.00731.001).

